PHYSICAL REVIEW A **78**, 062713 (2008)

Phase-index problem in the semiclassical description of molecular collisions

L. Bonnet[*] and C. Crespos

Institut des Sciences Moléculaires, Université Bordeaux 1, 351 Cours de la Libération, 33405 Talence Cedex, France

(Received 22 October 2008; published 17 December 2008; corrected 23 December 2008)

Semiclassical approaches of molecular collisions as proposed by Miller and Marcus involve phase indices, related to focal and turning points along trajectories contributing to *S* matrix elements. The main purpose of the work is to revisit the previous approaches in the case of two degrees of freedom rotationally inelastic collisions so as to make phase indices explicitly appear from first principles. Classical *S* matrix theory (CSMT) and three semiclassical initial value representation (SCIVR) treatments, respectively involving simple, double, and triple integrals, are considered. The phase index is either the Maslov index of the classical configuration space Green function (CSMT and the first two SCIVR methods), or the Maslov index of the Van Vleck–Gutzwiller space-time propagator (third SCIVR method). In order to assess the validity of the four previous approaches, their predictions are compared with exact quantum scattering results for interaction potentials leading to strong quantum interferences. The Gaussian weighting procedure, recently introduced in the quasiclassical trajectory method, is used here for practical CSMT calculations. We finally discuss the standard application of CSMT in the light of the previous developments and results.

DOI: 10.1103/PhysRevA.78.062713 PACS number(s): 34.10.+x, 31.15.xg, 34.50.Lf

I. INTRODUCTION

State resolved integral and differential cross sections as well as rate constants of molecular collisions can be expressed in terms of scattering *S* matrix elements which play, therefore, a central role in the description of molecular reaction dynamics [1].

Assuming that for a given process, the electronic problem has been solved within the Born-Oppenheimer approximation so the interaction forces between nuclei are known [2–5], state-of-the-art descriptions of *S* matrix elements are in principle performed within the framework of exact quantum scattering (EQS) approaches [6–13]. However, despite the impressive progress of computer performances achieved in the last three decades, these approaches can hardly be applied to more than three-atom systems as the basis sizes necessary for converging the calculations are usually prohibitive.

A popular alternative is the quasiclassical trajectory (QCT) method [14–16]. It is intuitive, easy to implement, much less time consuming than EQS approaches and for the latter reason, applicable to complex processes involving polyatomic species. However, the QCT method does only provide an estimation of the moduli of *S* matrix elements, not their phases. In addition to that, there is no guarantee on the accuracy of the former when interference effects are strong. For such reasons, the QCT method may lead to rather poor predictions.

By the end of the 1960s, QCT calculations on realistic triatomic reactions were almost routine [17,18] while EQS calculations could only be done for inelastic collisions in reduced dimensionality [19]. Pioneering works were then performed in the early 1970s by Miller [20–33] and Marcus [34–47] in order to develop semiclassical descriptions of molecular collisions combining the conceptual and numerical advantages of classical mechanics with the quantum principle of superposition. These works led to *classical S matrix theory* (CSMT) and the first *semiclassical initial value representation* (SCIVR) treatments [21,35] which had profound influences on the understanding of molecular collisions [48–50].

After a few applications [21,32,51–53], these approaches were nearly abandoned in the late 1970s, mainly because the increase of computing power at that time led many people to develop EQS treatments. Two decades later, however, the patent limitation of the applicability of EQS methods to small systems triggered off a strong rebirth of interest for semiclassical approaches with the hope to apply them to polyatomic processes in the relatively near future. But basic problems inherent to the semiclassical description should first be solved or clarified. In this paper, we focus our attention on one of them, the *phase index problem*.

The phase index, related to the number of catastrophes (focal and/or turning points) encountered along classical paths (see Sec. III), is crucial for an accurate description of interference effects [54–56]. This index is generally called the *Maslov index*, in honor of Maslov who did basic research in semiclassical mechanics in the 1960s [57]. We shall indifferently call it the phase or Maslov index in the following.

Though initially, the Maslov index was not explicitly taken into account in CSMT and SCIVR treatments, it was finally added to these formulations [43,47,58–61]. However, it seems to us, after many difficult readings, that it was more an *ad hoc* addition suggested by previous standard works on propagators and Green functions [54–56] than a correction arising from first-principle derivations [62]. The aim of the present work is to perform such derivations for a rotationally inelastic collision involving two degrees of freedom. We indeed believe that putting semiclassical collision theory on as firm theoretical grounds as is possible increases the chances for its successful application to realistic molecular collisions. The reasons for choosing the previous model system are discussed at the end of the work (see Sec. IX).

---

[*] Corresponding author. l.bonnet@ism.u-bordeaux1.fr

The spirit of our approach is the following: Miller showed how S matrix elements can be expressed in terms of the Green function in configuration space [32]. Besides, in his seminal theory on energy spectrum according to classical mechanics, Gutzwiller derived the classical limit of the previous Green function which involves a clearly defined phase index [54–56,63]. By combining the two previous works, we show that the indices appearing in CSMT and the one-dimensional (1D) and 2D SCIVR approaches respectively involving one- and two-dimensional integrals are all equal to the Maslov index of the Green function. The proof is achieved within the central approximation of semiclassical mechanics, i.e., the *stationary phase approximation* (SPA) [54–56]. For completeness, we also consider the 3D SCIVR approach of Skinner and Miller [64,65] for which the phase index is now the Maslov index of the Van Vleck–Gutzwiller space-time propagator [54–56].

We are aware of efficient SCIVR theories using either the Herman-Kluk propagator [66,67] or alternative ideas [68–70] and avoiding the Maslov index issue. However, our main objective is to arrive at a clear derivation of CSMT, for the latter played a central role in the derivation of the recent and promising Gaussian weighted trajectory (GWT) method [71–73]. This approach was indeed applied to several realistic triatomic processes (never studied by an alternative semiclassical treatment) and the state resolved integral cross sections predicted were found to be in good to close agreement with EQS and experimental results [74–77]. Since CSMT might keep playing a key role in the development of the GWT method, contributing to the strengthening of its basis seems important to us. The study of the three previously mentioned SCIVR approaches is then in the logical continuity of the previous contribution.

The paper is organized as follows. The system of interest is presented in Sec. II. CSMT is revisited in Sec. III and the three SCIVR treatments of interest are derived in Secs. IV–VI. The exact time-dependent quantum scattering approach used to check the validity of the previous semiclassical treatments is presented in Sec. VII. Semiclassical and quantum predictions are compared and discussed in Sec. VIII in the case of interaction potentials leading to strong quantum interferences. The application of CSMT to vibrationally inelastic and reactive processes is briefly discussed in Sec. IX and Sec. X concludes.

II. SYSTEM OF INTEREST

We consider the collision between atom A and the rigid diatom BC, at the end of which the rotational state of the diatom may have changed. Both A and the center of mass G of BC are supposed to lie on a fixed x axis of the laboratory frame. The system is represented in Fig. 1. The space coordinates of the problem are R, the distance between A and G, and ϕ, the angle between the x axis and **BC** (bold symbols are used for vectors throughout this work). The conjugate momenta of R and ϕ are P and J, respectively. The four previous coordinates form a set of canonical variables satisfying the Hamilton equations [78–80]

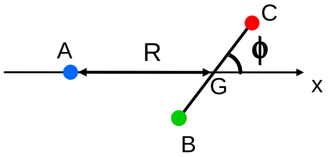

FIG. 1. (Color online) Molecular system considered in this work.

$$\dot{R} = \frac{\partial H}{\partial P}, \quad \dot{P} = -\frac{\partial H}{\partial R} \tag{1}$$

and

$$\dot{\phi} = \frac{\partial H}{\partial J}, \quad \dot{J} = -\frac{\partial H}{\partial \phi}. \tag{2}$$

H is the classical Hamiltonian given by

$$H = T + V \tag{3}$$

with

$$T = \frac{P^2}{2\mu} + \frac{J^2}{2I}. \tag{4}$$

T is the kinetic energy and $V \equiv V(R,\phi)$ is the interaction potential energy, different from zero when A and BC are sufficiently close the one to each other (a few Å). μ is the reduced mass of A with respect to BC and I is the moment of inertia of BC. I is equal to mr^2 where m and r are the reduced mass and length of BC, respectively. Given that $P=\mu\dot{R}$ and $J=I\dot{\phi}$ [see the left side of Eqs. (1) and (2)], T also reads

$$T = \frac{1}{2}(\mu\dot{R}^2 + I\dot{\phi}^2) \tag{5}$$

or

$$T = \frac{1}{2}(P\dot{R} + J\dot{\phi}). \tag{6}$$

The atom-diatom system being isolated,

$$H = E \tag{7}$$

at any instant, E being the total energy of the process.

The Lagrangian of the system is

$$L = 2T - H. \tag{8}$$

The developments of the next section will show the interest of considering the scaled variable

$$r = \left(\frac{\mu}{I}\right)^{1/2} R \tag{9}$$

rather than R itself. From Eqs. (3), (5), (8), and (9) and given that the conjugate momentum p of r is defined by [78,79]

$$p = \frac{\partial L}{\partial \dot{r}}, \tag{10}$$

we arrive at

$$p = I\dot{r} = \left(\frac{I}{\mu}\right)^{1/2} P. \tag{11}$$

The kinetic terms (4)–(6) read then

$$T = \frac{p^2 + J^2}{2I}, \tag{12}$$

$$T = \frac{I}{2}(\dot{r}^2 + \dot{\phi}^2) \tag{13}$$

and

$$T = \frac{1}{2}(p\dot{r} + J\dot{\phi}), \tag{14}$$

respectively.

The initial collision energy is denoted E_c. BC starts in the rotational state $|j_1\rangle$ and ends in the analogous state $|j_2\rangle$. Their associated wave functions are

$$\langle\phi|j_k\rangle = \varphi_k(\phi) = \frac{1}{(2\pi)^{1/2}} e^{ij_k\phi}, \tag{15}$$

$k=1,2$.

We note that J is a classical angular momentum while j_1 and j_2 are quantum numbers.

E, E_c, and j_1 are related by

$$E = E_c + \frac{\hbar^2 j_1(j_1+1)}{2I}. \tag{16}$$

III. FROM SPACE-TIME PROPAGATOR TO *S* MATRIX ELEMENTS

A. From Miller to Gutzwiller

1. S matrix elements and Green function

The S matrix element $S_{j_2 j_1}(E)$ is defined as the probability amplitude that BC starts in $|j_1\rangle$ and ends in $|j_2\rangle$. Its square modulus gives the final rotational state population $P_{j_2 j_1}(E)$ which is the essential observable of the process of interest.

Miller showed in the framework of formal collision theory that $S_{j_2 j_1}(E)$ can be written as [32]

$$S_{j_2 j_1}(E) = a\int_0^{+\infty} dt e^{iEt/\hbar}\langle R_2 j_2|e^{-i\hat{H}t/\hbar}|R_1 j_1\rangle \tag{17}$$

with

$$a = \frac{|\Pi_1\Pi_2|^{1/2}}{i\mu} e^{i(\Pi_1 R_1 - \Pi_2 R_2)/\hbar} \tag{18}$$

(this expression only differs from Miller's one [32] by the irrelevant phase factor i). Both R_1 and R_2 have infinite values (a few tens of Å in practice). $\hat{H}$ is the Hamiltonian operator deduced from Eq. (3) by the correspondence principle (see Sec. VII). t is time and $\hbar$ is Planck constant divided by 2π. The quantity

$$\Pi_1 = -(2\mu E_c)^{1/2} = -\left[2\mu\left(E - \frac{\hbar^2 j_1(j_1+1)}{2I}\right)\right]^{1/2} \tag{19}$$

is the initial value of the translational momentum while the quantity

$$\Pi_2 = \left[2\mu\left(E - \frac{\hbar^2 j_2(j_2+1)}{2I}\right)\right]^{1/2} \tag{20}$$

is the final value consistent with j_2.

We shall now use r instead of R in the S matrix element (17). This amounts to replace there the propagator $\langle R_2 j_2|e^{-i\hat{H}t/\hbar}|R_1 j_1\rangle$ by its expression in terms of $\langle r_2 j_2|e^{-i\hat{H}t/\hbar}|r_1 j_1\rangle$. To this aim, let us consider the wave packet $\Psi(R,t)$ satisfying the standard relation

$$\Psi(R_2,t) = \int dR_1\langle R_2|e^{-i\hat{H}t/\hbar}|R_1\rangle\Psi(R_1,0). \tag{21}$$

Setting

$$\psi(r,t) = \Psi(R,t), \tag{22}$$

we have from Eqs. (9) and (21)

$$\psi(r_2,t) = \int dr_1\left(\frac{I}{\mu}\right)^{1/2}\langle R_2|e^{-i\hat{H}t/\hbar}|R_1\rangle\psi(r_1,0). \tag{23}$$

Now, given that

$$\psi(r_2,t) = \int dr_1\langle r_2|e^{-i\hat{H}t/\hbar}|r_1\rangle\psi(r_1,0), \tag{24}$$

we arrive at

$$\langle R_2|e^{-i\hat{H}t/\hbar}|R_1\rangle = \left(\frac{\mu}{I}\right)^{1/2}\langle r_2|e^{-i\hat{H}t/\hbar}|r_1\rangle. \tag{25}$$

Equation (17) can thus be rewritten as

$$S_{j_2 j_1}(E) = b\int_0^{+\infty} dt e^{iEt/\hbar}\langle r_2 j_2|e^{-i\hat{H}t/\hbar}|r_1 j_1\rangle \tag{26}$$

with

$$b = \left(\frac{\mu}{I}\right)^{1/2} a. \tag{27}$$

By using the closure relation

$$1 = \int d\phi_k|\phi_k\rangle\langle\phi_k|, \tag{28}$$

$k=1,2$, the propagator $\langle r_2 j_2|e^{-i\hat{H}t/\hbar}|r_1 j_1\rangle$ can be expressed in terms of the space-time propagator $\langle r_2\phi_2|e^{-i\hat{H}t/\hbar}|r_1\phi_1\rangle$ as

$$\langle r_2 j_2|e^{-i\hat{H}t/\hbar}|r_1 j_1\rangle = \int d\phi_2 d\phi_1\langle j_2|\phi_2\rangle\langle r_2\phi_2|e^{-i\hat{H}t/\hbar}|r_1\phi_1\rangle \times\langle\phi_1|j_1\rangle. \tag{29}$$

From Eqs. (26) and (29), $S_{j_2 j_1}(E)$ may then be rewritten as

$$S_{j_2j_1}(E) = b \int d\phi_2 d\phi_1 \langle j_2|\phi_2\rangle\langle\phi_1|j_1\rangle G(\phi_2,\phi_1|r_2,r_1,E) \tag{30}$$

where

$$G(\phi_2,\phi_1|r_2,r_1,E) = \int_0^{+\infty} dt e^{iEt/\hbar}\langle r_2\phi_2|e^{-i\hat{H}t/\hbar}|r_1\phi_1\rangle \tag{31}$$

is the Green function.

2. Classical Green function

The Van Vleck–Gutzwiller semiclassical approximation of the space-time propagator $\langle r_2\phi_2|e^{-i\hat{H}t/\hbar}|r_1\phi_1\rangle$ is [54–56,63]

$$\langle r_2\phi_2|e^{-i\hat{H}t/\hbar}|r_1\phi_1\rangle_{sc} = \sum_{Traj} \frac{|\Delta|^{1/2}}{2\pi i\hbar} e^{i(W/\hbar-\pi\kappa/2)}, \tag{32}$$

where

$$\Delta = \det(M_t), \tag{33}$$

$$M_t = \begin{pmatrix} -\dfrac{\partial^2 W}{\partial r_t \partial r_1} & -\dfrac{\partial^2 W}{\partial r_t \partial \phi_1} \\ -\dfrac{\partial^2 W}{\partial \phi_t \partial r_1} & -\dfrac{\partial^2 W}{\partial \phi_t \partial \phi_1} \end{pmatrix}, \tag{34}$$

$$W = \int_0^t d\tau L \tag{35}$$

and the index κ is the sum of the numbers of time each eigenvalue of M_τ^{-1} changes sign when τ runs from 0 to t. Note that within the above notations, $r_\tau = r_1$ and $\phi_\tau = \phi_1$ when $\tau = 0$ while $r_\tau = r_2$ and $\phi_\tau = \phi_2$ when $\tau = t$. At the instant when κ increases by one unit (or two, but very rarely), the trajectory touches a so-called caustic and Δ diverges [54–56]. The sum is over the whole set of classical paths going from (r_1,ϕ_1) to (r_2,ϕ_2) in the period of time t. W, the time integral of the Lagrangian given by Eqs. (3), (8), and (14), is the usual action integral [78,79].

With κ kept at zero, propagator (32) is the celebrated Van Vleck semiclassical propagator (reduced to one term only). However, this propagator is only valid for the short times where the first caustic has not been touched. Beyond the latter, neglecting κ does not allow for a correct treatment of interference effects. The crucial addition of κ is due to Gutzwiller [63], Pechukas having also contributed a few times later to its introduction [81]. More details on κ and its equivalent in momentum or mixed spaces can be found in [54–56,82–87].

A second basic contribution from Gutzwiller [63] was the derivation of the classical Green function within the SPA introduced in the next subsection. This derivation consists in replacing in Eq. (31) the exact propagator by its approximation (32) and performing the integration with respect to time within the SPA. The final result is

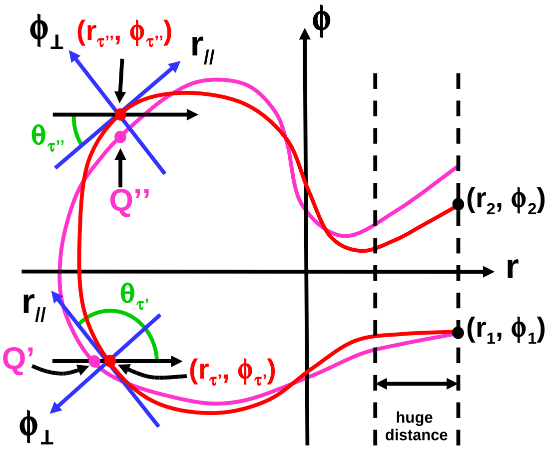

FIG. 2. (Color online) A given classical path in the (r,ϕ) plane goes from (r_1,ϕ_1) to (r_2,ϕ_2) at the energy E. A neighboring path of energy E is also shown, which has in (r_1,ϕ_1) a slightly different direction. The running point of the first path is represented twice by the intermediate positions $(r_{\tau'},\phi_{\tau'})$ and $(r_{\tau''},\phi_{\tau''})$ corresponding to the instants τ' and τ''. The local coordinate system $(r_\parallel,\phi_\perp)$ at these points is represented. More details are given in the text. We note that the scale along the r coordinate is not linear, the distance between the dashed curves being huge.

$$G(\phi_2,\phi_1|r_2,r_1,E)_{sc} = \frac{1}{(2\pi i\hbar)^{1/2}} \sum_{Traj} \left| \frac{1}{\dot{r}_{\parallel 1}\dot{r}_{\parallel 2}} \frac{\partial J_{\perp 1}}{\partial \phi_{\perp 2}}\bigg|_{\phi_{\perp 1}} \right|^{1/2} e^{i(\Omega/\hbar-\pi\eta/2)}. \tag{36}$$

The sum is now over the whole set of classical paths going from (r_1,ϕ_1) to (r_2,ϕ_2) at the energy E and in a period of time $t \equiv t(\phi_2,\phi_1|r_2,r_1,E)$. For each path, a local orthonormal coordinate system $(r_\parallel,\phi_\perp)$ such as the one represented in Fig. 2 is used. In addition to the reference path from (r_1,ϕ_1) to (r_2,ϕ_2), a neighboring path of energy E is considered, which starts from (r_1,ϕ_1) in a slightly different direction. The running point of the reference path is represented twice by the intermediate positions $(r_{\tau'},\phi_{\tau'})$ and $(r_{\tau''},\phi_{\tau''})$ corresponding to the instants τ' and τ''. The local coordinate system $(r_\parallel,\phi_\perp)$ at these points is represented. The $r_\parallel$ axis is tangential to the trajectory and makes the angles $\theta_{\tau'}$ and $\theta_{\tau''}$ with the r axis in $(r_{\tau'},\phi_{\tau'})$ and $(r_{\tau''},\phi_{\tau''})$. The running point of the neighboring path is also represented twice by Q' and Q'' corresponding to τ' and τ'', respectively. While the running point of the reference trajectory is, by definition, always at the origin of the local frame, we clearly see that the running point of the neighboring path moves in the local frame. Q' is for instance in the positive quadrant while Q'' is in the negative one. Last but not least, the convention adopted here is that the local frame is fixed in (r,ϕ). As a consequence, the velocities along the two previous paths is the same in (r,ϕ) and $(r_\parallel,\phi_\perp)$. More details on this local frame are given further below.

$\dot{r}_{\parallel 1}$ and $\dot{r}_{\parallel 2}$ in Eq. (36) are the moduli of the velocity vectors in (r_1,ϕ_1) and (r_2,ϕ_2), respectively. $\partial J_{\perp 1}/\partial\phi_{\perp 2}|_{\phi_{\perp 1}}$ is the inverse ratio of the first derivative of $\phi_\perp$ in (r_2,ϕ_2) with respect to $J_\perp$ in (r_1,ϕ_1) for fixed values of $\phi_{\perp 1}$ and the energy E (see further below for the practical evaluation of this quantity). Ω is a new action integral related to W by the Legendre transformation

$$\Omega = W + Et. \tag{37}$$

From Eqs. (6), (8), (14), (7), and (35), Ω is found to be given by

$$\Omega = \int_0^t d\tau (P\dot{R} + J\dot{\phi}) = \int_0^t d\tau (p\dot{r} + J\dot{\phi}). \tag{38}$$

The index η is equal to the number of times the trajectory touches a caustic or a turning point, i.e., the number of times the derivative $\partial\phi_{\perp\tau}/\partial J_{\perp 1}|_{\phi_{\perp 1}}$ changes sign between (r_1,ϕ_1) $(\tau=0)$ and (r_2,ϕ_2) $(\tau=t)$. An alternative and insightful derivation of Eq. (36) was given by Möhring *et al.* [88].

In the following, we shall replace the Green function in Eq. (30) by its classical limit (36) and perform the double integral with respect to ϕ_2 and ϕ_1 within the SPA. This will lead to the Miller-Marcus expression of classical S matrix elements with a clear definition of phase indices.

Before doing that, we spend some time on the practical calculation of η which will prove to play a central role in the determination of $S_{j_2 j_1}(E)$.

3. Practical calculation of η

A practical calculation of η requiring the propagation of the monodromy matrix is, for instance, given by Eckhardt and Wintgen [89]. However, we shall use here a more pedestrian approach that we have found interesting from the numerical point of view.

It is clear from Fig. 2 that the transformation between the local orthonormal frame $(r_\parallel,\phi_\perp)$ and the initial frame (r,ϕ) at the particular instant $t=\tau$ is given by

$$\begin{pmatrix} r - r_\tau \\ \phi - \phi_\tau \end{pmatrix} = \begin{pmatrix} \cos\theta_\tau & -\sin\theta_\tau \\ \sin\theta_\tau & \cos\theta_\tau \end{pmatrix} \begin{pmatrix} r_\parallel \\ \phi_\perp \end{pmatrix}. \tag{39}$$

As previously stated, (r_τ,ϕ_τ) is chosen to be the origin of the local frame. The velocity vector being $(\dot{r}_\tau,\dot{\phi}_\tau)$, the angle θ_τ between the r axis and the $r_\parallel$ axis is defined by (see Fig. 2)

$$\cos\theta_\tau = \frac{\dot{r}_\tau}{(\dot{r}_\tau^2+\dot{\phi}_\tau^2)^{1/2}} = \frac{p_\tau}{(p_\tau^2+J_\tau^2)^{1/2}} \tag{40}$$

and

$$\sin\theta_\tau = \frac{\dot{\phi}_\tau}{(\dot{r}_\tau^2+\dot{\phi}_\tau^2)^{1/2}} = \frac{J_\tau}{(p_\tau^2+J_\tau^2)^{1/2}}. \tag{41}$$

The second equalities come from the fact that $p_\tau = I\dot{r}_\tau$ and $J_\tau = I\dot{\phi}_\tau$.

The local frame being supposed to be fixed, r_τ, ϕ_τ, and θ_τ in Eq. (39) are now considered as time-independent parameters. From Eqs. (13) and (39), we have thus

$$T = \frac{I}{2}(\dot{r}_\parallel^{\,2} + \dot{\phi}_\perp^{\,2}) \tag{42}$$

and using Eqs. (3) and (8), and the basic relations [78,79]

$$p_\parallel = \frac{\partial L}{\partial \dot{r}_\parallel}, \quad J_\perp = \frac{\partial L}{\partial \dot{\phi}_\perp}, \tag{43}$$

giving the conjugate momenta of $r_\parallel$ and $\phi_\perp$, we arrive at

$$\begin{pmatrix} p \\ J \end{pmatrix} = \begin{pmatrix} \cos\theta_\tau & -\sin\theta_\tau \\ \sin\theta_\tau & \cos\theta_\tau \end{pmatrix} \begin{pmatrix} p_\parallel \\ J_\perp \end{pmatrix} \tag{44}$$

and

$$T = \frac{p_\parallel^2 + J_\perp^2}{2I}. \tag{45}$$

As previously stated, the initial value r_1 of r is very large (infinite in principle). At time zero therefore V is zero and $T=E$. By construction, $J_{\perp 1}=0$ and from Eq. (45),

$$p_{\parallel 1} = (2IE)^{1/2}. \tag{46}$$

Similar arguments lead to

$$p_{\parallel 2} = (2IE)^{1/2}. \tag{47}$$

We wish now to calculate the quantity $\partial\phi_{\perp\tau}/\partial J_{\perp 1}|_{\phi_{\perp 1}}$ whose number of zeros between (r_1,ϕ_1) and (r_2,ϕ_2) is just η. We shall therefore consider a second trajectory starting from (r_1,ϕ_1) with $J_\perp = \delta J_{\perp 1}$, instead of $J_\perp = J_{\perp 1}=0$. However, the second path has to be on the energy shell $H=E$ as well (η is the Maslov index in the time-independent representation). Since this path starts from the same configuration space point, the kinetic energy T [see Eq. (45)] must be the same for both paths. The second trajectory should thus start with $p_{\parallel 1}+\delta p_{\parallel 1}$ satisfying

$$(p_{\parallel 1} + \delta p_{\parallel 1})^2 + \delta J_{\perp 1}^2 = p_{\parallel 1}^2 \tag{48}$$

leading to

$$\delta p_{\parallel 1} \approx -\frac{\delta J_{\perp 1}^2}{2p_{\parallel 1}} \tag{49}$$

when neglecting $\delta p_{\parallel 1}$ with respect to $p_{\parallel 1}$. Equations (46) and (49) prove that $\delta p_{\parallel 1}$ is always negligible with respect to $\delta J_{\perp 1}$. We may thus start the second trajectory with $p_{\parallel 1}$ and $\delta J_{\perp 1}$ (instead of $p_{\parallel 1}+\delta p_{\parallel 1}$ and $\delta J_{\perp 1}$). The initial dynamical situation is depicted in Fig. 3.

Let us now express the initial conditions of the pair of trajectories in the original (R,ϕ,P,J) phase space where we shall run trajectories in practice. For the reference path, these conditions are (R_1,ϕ_1,P_1,J_1) and for the neighboring path, we shall call them $(R_{n1},\phi_{n1},P_{n1},J_{n1})$. From Eqs. (11), (12), (40), and (41), and the fact that $T=E$, the value θ_1 of θ at time zero is completely specified by

$$\cos\theta_1 = \frac{P_1}{(2\mu E)^{1/2}} \tag{50}$$

and

$$\sin\theta_1 = \frac{J_1}{(2IE)^{1/2}}. \tag{51}$$

Similar arguments lead to

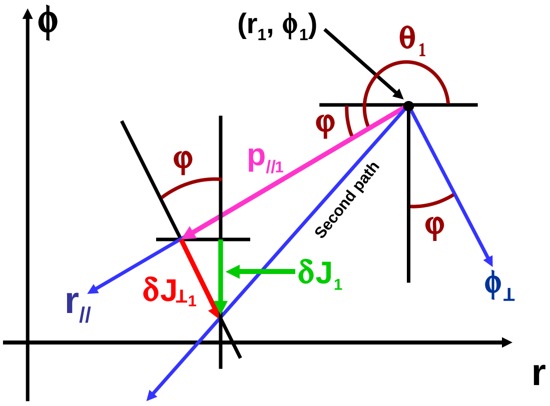

FIG. 3. (Color online) Initial dynamical conditions of the reference trajectory and a neighboring one in the fixed frame (r,ϕ) and in the local frame $(r_\parallel,\phi_\perp)$. Both paths start from the point (r_1,ϕ_1) of the frame (r,ϕ), also origin of the frame $(r_\parallel,\phi_\perp)$. The reference path, with initial momentum vector $\mathbf{p}_{\parallel 1}$, is along the $r_\parallel$ axis while the second path, with initial momentum vector $\mathbf{p}_{\parallel 1}+\delta\mathbf{J}_{\perp 1}$, makes with the previous path an infinitesimal angle. The relevant angles θ_1 and φ are shown as well as the projection $\delta\mathbf{J}_1$ of $\delta\mathbf{J}_{\perp 1}$ on the ϕ axis. We note that in the present case, δJ_1 is negative.

$$\cos\theta_2 = \frac{P_2}{(2\mu E)^{1/2}}. \tag{52}$$

Since both paths start from the same configuration space point, $R_{n1}=R_1$ and $\phi_{n1}=\phi_1$. From Eq. (11), Eq. (44) with $p_\parallel$ replaced by $(2IE)^{1/2}$ [see Eq. (46)] and $J_\perp$ replaced by $\delta J_{\perp 1}$ and from Eqs. (50) and (51), we arrive at

$$P_{n1} = P_1 - \left(\frac{\mu}{2E}\right)^{1/2}\frac{\delta J_{\perp 1}}{I}J_1 \tag{53}$$

and

$$J_{n1} = \frac{\delta J_{\perp 1}}{(2\mu E)^{1/2}}P_1 + J_1. \tag{54}$$

The two classical paths are then run according to standard numerical methods [14–16], thus giving $(R_\tau,\phi_\tau,P_\tau,J_\tau)$ and $(R_{n\tau},\phi_{n\tau},P_{n\tau},J_{n\tau})$. $\delta\phi_{\perp\tau}$ deduced from Eqs. (9), (40), and (41), and the inverse of Eq. (39), reads

$$\delta\phi_{\perp\tau} = -\sin\theta_\tau\left(\frac{\mu}{I}\right)^{1/2}(R_{n\tau}-R_\tau)+\cos\theta_\tau(\phi_{n\tau}-\phi_\tau) \tag{55}$$

with

$$\cos\theta_\tau = \frac{(I/\mu)^{1/2}P_\tau}{(IP_\tau^2/\mu+J_\tau^2)^{1/2}} \tag{56}$$

and

$$\sin\theta_\tau = \frac{J_\tau}{(IP_\tau^2/\mu+J_\tau^2)^{1/2}}. \tag{57}$$

The expected number η of zeros of $\partial\phi_{\perp\tau}/\partial J_{\perp 1}|_{\phi_{\perp 1}}$ between $\tau=0$ and $\tau=t$ is finally given by the number of zeros of $\delta\phi_{\perp\tau}$ during the same period of time, in the limit where $\delta J_{\perp 1}$ tends to zero in Eqs. (53) and (54).

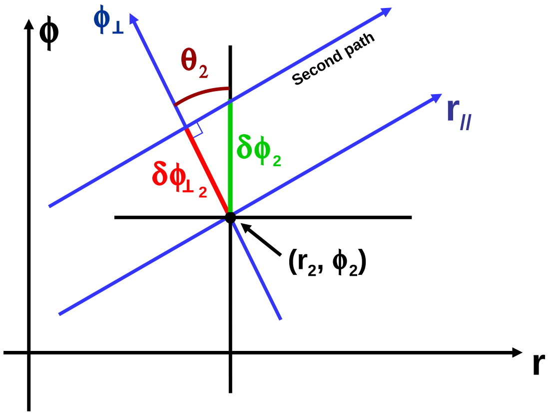

FIG. 4. (Color online) Final dynamical conditions of the reference trajectory and a neighboring one in the fixed frame (r,ϕ) and in the local frame $(r_\parallel,\phi_\perp)$. The reference path runs through the point (r_2,ϕ_2) while the second path is parallel to the reference path in the limit where $\delta J_{\perp 1}$ tends to zero. The angle θ_2 is shown as well as the infinitesimal angular differences $\delta\phi_2$ and $\delta\phi_{\perp 2}$.

B. From Gutzwiller to Miller and Marcus

The goal of the present section is to recover the CSMT expression of Miller and Marcus from the classical Green function of Gutzwiller with a clear definition of the phase index. To achieve this goal, we have to replace the Green function in Eq. (30) by its classical limit (36) and perform the double integral with respect to ϕ_2 and ϕ_1 within the SPA. A few considerations, however, are first necessary.

1. From local to fixed frame derivatives

As a first step, we wish to express $\partial\phi_{\perp 2}/\partial J_{\perp 1}|_{\phi_{\perp 1}}$ in Eq. (36) in terms of ϕ_2 and ϕ_1. This is a simple matter if we note from Figs. 3 and 4 that

$$\delta J_1 = -\cos\varphi\,\delta J_{\perp 1} \tag{58}$$

(the minus sign comes from the fact that δJ_1 is negative) and

$$\delta\phi_{\perp 2} = \cos\theta_2\,\delta\phi_2. \tag{59}$$

Since

$$\varphi = \theta_1 - \pi, \tag{60}$$

we arrive at

$$\left.\frac{\partial\phi_{\perp 2}}{\partial J_{\perp 1}}\right|_{\phi_{\perp 1}} = \cos\theta_1\cos\theta_2\left.\frac{\partial\phi_2}{\partial J_1}\right|_{\phi_1}. \tag{61}$$

We have thus related the partial derivative in the local frame to its analog in the fixed frame.

From Eqs. (50) and (52), and owing to the fact that

$$J_1 = -\left.\frac{\partial\Omega}{\partial\phi_1}\right|_{\phi_2} \tag{62}$$

[this standard relation comes directly from Eq. (38)], Eq. (61) finally reads

$$\left.\frac{\partial\phi_{\perp 2}}{\partial J_{\perp 1}}\right|_{\phi_{\perp 1}} = -\frac{P_1P_2}{2\mu E}\left(\frac{\partial^2\Omega}{\partial\phi_2\partial\phi_1}\right)^{-1}. \tag{63}$$

For fixed values of the parameters r_2, r_1 and E, P_1, P_2, and Ω are completely specified by ϕ_2 and ϕ_1 as well as the trajectory number if several trajectories go from (r_1,ϕ_1) to (r_2,ϕ_2) at E. The expected link between $\partial\phi_{\perp 2}/\partial J_{\perp 1}|_{\phi_{\perp 1}}$ and the integration variables ϕ_2 and ϕ_1 is thus clearly determined.

2. Applying the stationary phase approximation

A few more manipulations before applying the SPA may help to clarify the developments. From Eqs. (3), (8), and (42), and the left identity of Eq. (43),

$$p_{\parallel} = I\dot{r}_{\parallel}, \tag{64}$$

which, together with Eq. (46), leads to

$$\dot{r}_{\parallel 1} = (2E/I)^{1/2}. \tag{65}$$

Similar arguments and Eq. (47) lead to

$$\dot{r}_{\parallel 2} = (2E/I)^{1/2}. \tag{66}$$

Taking into account these expressions as well as Eq. (63) in Eqs. (30) and (36) leads to

$$S_{j_2j_1}(E) = \int d\phi_2 d\phi_1 c(\phi_2,\phi_1) d(\phi_2,\phi_1) \tag{67}$$

with

$$c(\phi_2,\phi_1) = \frac{1}{(2\pi i\hbar)^{1/2}}\frac{1}{2\pi i}e^{i(\Pi_1R_1-\Pi_2R_2+\hbar j_1\phi_1-\hbar j_2\phi_2)/\hbar} \tag{68}$$

and

$$d(\phi_2,\phi_1) = \sum_{Traj}\left|\frac{\Pi_1\Pi_2}{P_1P_2}\frac{\partial^2\Omega}{\partial\phi_2\partial\phi_1}\right|^{1/2} e^{i(\Omega/\hbar-\pi\eta/2)}. \tag{69}$$

We are now ready to perform, within the SPA, the double integration with respect to ϕ_2 and ϕ_1 in Eq. (30), or equivalently, in Eq. (67).

With f being a function of two variables x and y and s a sufficiently small parameter, the SPA states that

$$\int dxdy e^{if(x,y)/s} \approx \sum_k \frac{2\pi i s}{|\Delta_k|^{1/2}} e^{i(f_k/s-\pi\nu_k/2)}, \tag{70}$$

where (x_k,y_k) is the kth stationary point of f, $f_k = f(x_k,y_k)$,

$$\Delta_k = \det(M_k), \tag{71}$$

$$M_k = \begin{pmatrix} \left.\frac{\partial^2 f}{\partial x^2}\right|_k & \left.\frac{\partial^2 f}{\partial x\partial y}\right|_k \\ \left.\frac{\partial^2 f}{\partial x\partial y}\right|_k & \left.\frac{\partial^2 f}{\partial y^2}\right|_k \end{pmatrix}, \tag{72}$$

and ν_k is the number of negative eigenvalues of M_k [54–56].

Equations (70)–(72) are obtained by limiting f to its second order development around the stationary points. For sufficiently small values of s, the rate of oscillation of the phase $\exp(if(x,y)/s)$ increases so much with the distance from a stationary point that only the close neighborhoods of stationary points significantly contribute to the phase integral. The SPA is thus a good approximation only whether the second order development of f is valid in the previous neighborhoods. In the contrary case, it is necessary to consider higher order developments of f leading to expressions differing from Eqs. (70)–(72). We shall not do this in the present work, however, for the SCIVR approaches presented in Secs. IV–VI allow us to go around this difficulty in a satisfying and simpler way.

In Eqs. (67)–(69), the small parameter s is of course $\hbar$ and as far as applying the SPA is concerned, the relevant part of the phase is

$$f(\phi_2,\phi_1) = \Omega + \hbar j_1\phi_1 - \hbar j_2\phi_2. \tag{73}$$

The stationary phase condition defines the values ϕ_{2k} and ϕ_{1k} of ϕ_2 and ϕ_1 contributing to $S_{j_2j_1}(E)$. These values satisfy the relations

$$\hbar j_2 = \left.\frac{\partial\Omega}{\partial\phi_2}\right|_{\phi_1}(\phi_{2k},\phi_{1k}) \tag{74}$$

and

$$\hbar j_1 = -\left.\frac{\partial\Omega}{\partial\phi_1}\right|_{\phi_2}(\phi_{2k},\phi_{1k}). \tag{75}$$

Now, from Eq. (62) and its companion

$$J_2 = \left.\frac{\partial\Omega}{\partial\phi_2}\right|_{\phi_1} \tag{76}$$

[just as Eq. (62), this standard relation comes from Eq. (38)], it appears quite clearly that Eqs. (74) and (75) define classical paths starting from (R_1,ϕ_{1k}) with

$$J_1 = \hbar j_1 \tag{77}$$

and

$$P_1 = -\left[2\mu\left(E - \frac{\hbar^2 j_1^2}{2I}\right)\right]^{1/2} = \pi_1 \tag{78}$$

and reaching (R_2,ϕ_{2k}) with

$$J_2 = \hbar j_2 \tag{79}$$

and

$$P_2 = \left[2\mu\left(E - \frac{\hbar^2 j_2^2}{2I}\right)\right]^{1/2} = \pi_2 \tag{80}$$

after visiting the interaction region. Equations (78) and (80) are deduced from Eqs. (4), (77), and (79) and the fact that in (R_1,ϕ_{1k}) and (R_2,ϕ_{2k}), $T=E$.

From Eqs. (67)–(80), we find

$$S_{j_2j_1}(E) = \left(\frac{\hbar}{2\pi i}\right)^{1/2} g\sum_k h_k o_k \tag{81}$$

with

$$g = \left|\frac{\Pi_1\Pi_2}{\pi_1\pi_2}\right|^{1/2} e^{i[(\Pi_1-\pi_1)R_1-(\Pi_2-\pi_2)R_2]/\hbar}, \tag{82}$$

$$h_k = \left| \frac{\left.\dfrac{\partial^2 \Omega}{\partial \phi_2 \partial \phi_1}\right|_k}{\det(M_k)} \right|^{1/2}, \tag{83}$$

$$M_k = \begin{pmatrix} \left.\dfrac{\partial^2 \Omega}{\partial \phi_2^2}\right|_k & \left.\dfrac{\partial^2 \Omega}{\partial \phi_2 \partial \phi_1}\right|_k \\ \left.\dfrac{\partial^2 \Omega}{\partial \phi_2 \partial \phi_1}\right|_k & \left.\dfrac{\partial^2 \Omega}{\partial \phi_1^2}\right|_k \end{pmatrix}, \tag{84}$$

$$o_k = e^{i[(\Omega_k + \pi_1 R_1 - \pi_2 R_2 + J_1 \phi_{1k} - J_2 \phi_{2k})/\hbar - \pi \chi_k/2]} \tag{85}$$

and

$$\chi_k = \eta_k + \nu_k. \tag{86}$$

ν_k is the number of negative eigenvalues of M_k, which can be rewritten as

$$M_k = \begin{pmatrix} \left.\dfrac{\partial J_2}{\partial \phi_2}\right|_{\phi_1}^{k} & -\left.\dfrac{\partial J_1}{\partial \phi_2}\right|_{\phi_1}^{k} \\ -\left.\dfrac{\partial J_1}{\partial \phi_2}\right|_{\phi_1}^{k} & -\left.\dfrac{\partial J_1}{\partial \phi_1}\right|_{\phi_2}^{k} \end{pmatrix} \tag{87}$$

when taking into account Eqs. (62) and (76). We shall come back to this index in the next section.

One notes that the summation Σ_{Traj} in Eq. (69) and the summation Σ_k for each trajectory due to the SPA (70) lead to an overall summation Σ_k in Eq. (81).

We shall now simplify h_k [see Eq. (83)]. We first note from Eqs. (62) and (87) that this quantity can be rewritten as

$$h_k = \left| \frac{- \left.\partial J_1/\partial \phi_2\right|_{\phi_1}^{k}}{\det(M_k)} \right|^{1/2} \tag{88}$$

with

$$\det(M_k) = - \left.\frac{\partial J_2}{\partial \phi_2}\right|_{\phi_1}^{k} \left.\frac{\partial J_1}{\partial \phi_1}\right|_{\phi_2}^{k} - \left(\left.\frac{\partial J_1}{\partial \phi_2}\right|_{\phi_1}^{k} \right)^2. \tag{89}$$

We next consider the first order developments

$$\phi_2 = \phi_{2k} + \left.\frac{\partial \phi_2}{\partial \phi_1}\right|_{J_1}^{k} (\phi_1 - \phi_{1k}) + \left.\frac{\partial \phi_2}{\partial J_1}\right|_{\phi_1}^{k} (J_1 - \hbar j_1) \tag{90}$$

and

$$J_2 = \hbar j_2 + \left.\frac{\partial J_2}{\partial \phi_1}\right|_{J_1}^{k} (\phi_1 - \phi_{1k}) + \left.\frac{\partial J_2}{\partial J_1}\right|_{\phi_1}^{k} (J_1 - \hbar j_1) \tag{91}$$

of ϕ_2 and J_2 in terms of ϕ_1 and J_1 around $(\phi_{1k}, \hbar j_1)$. For fixed values of R_1 and R_2 and given that

$$P_1 = - \left[2\mu \left(E - \frac{J_1^2}{2I} \right) \right]^{1/2}, \tag{92}$$

ϕ_2 and J_2 do only depend on ϕ_1 and J_1.

From Eq. (90), we get

$$\left.\frac{\partial J_1}{\partial \phi_1}\right|_{\phi_2}^{k} = - \left.\frac{\partial \phi_2}{\partial \phi_1}\right|_{J_1}^{k} \left.\frac{\partial J_1}{\partial \phi_2}\right|_{\phi_1}^{k}. \tag{93}$$

Replacing $(J_1 - \hbar j_1)$ in Eq. (91) by its expression in terms of ϕ_1 and ϕ_2 deduced from Eq. (90), we also find

$$\left.\frac{\partial J_2}{\partial \phi_2}\right|_{\phi_1}^{k} = \left.\frac{\partial J_2}{\partial J_1}\right|_{\phi_1}^{k} \left.\frac{\partial J_1}{\partial \phi_2}\right|_{\phi_1}^{k}; \tag{94}$$

$\det(M_k)$ [see Eq. (89)] can thus be rewritten as

$$\det(M_k) = \left(\left.\frac{\partial J_2}{\partial J_1}\right|_{\phi_1}^{k} \left.\frac{\partial \phi_2}{\partial \phi_1}\right|_{J_1}^{k} - 1 \right) \left(\left.\frac{\partial J_1}{\partial \phi_2}\right|_{\phi_1}^{k} \right)^2. \tag{95}$$

In addition to that, it is well known that for a two degrees of freedom system, the Hamiltonian flow is area preserving, by virtue of Liouville theorem [90]. Therefore $d\phi_2 dJ_2$ and $d\phi_1 dJ_1$ are equal, implying that

$$\begin{vmatrix} \left.\dfrac{\partial \phi_2}{\partial \phi_1}\right|_{J_1}^{k} & \left.\dfrac{\partial \phi_2}{\partial J_1}\right|_{\phi_1}^{k} \\ \left.\dfrac{\partial J_2}{\partial \phi_1}\right|_{J_1}^{k} & \left.\dfrac{\partial J_2}{\partial J_1}\right|_{\phi_1}^{k} \end{vmatrix} = 1. \tag{96}$$

Replacing 1 in Eq. (95) by the above Jacobian leads to

$$\det(M_k) = \left.\frac{\partial J_2}{\partial \phi_1}\right|_{J_1}^{k} \left.\frac{\partial J_1}{\partial \phi_2}\right|_{\phi_1}^{k}. \tag{97}$$

From Eqs. (88) and (97), h_k finally reads

$$h_k = \left| \left.\frac{\partial J_2}{\partial \phi_1}\right|_{J_1}^{k} \right|^{-1/2}. \tag{98}$$

Another route to demonstrate this result is to consider J_1 and J_2 as functions of ϕ_1 and ϕ_2 (instead of ϕ_2 and J_2 as functions of ϕ_1 and J_1). J_1 and J_2 are then given by the first order developments

$$J_1 = \hbar j_1 + \left.\frac{\partial J_1}{\partial \phi_1}\right|_{\phi_2}^{k} (\phi_1 - \phi_{1k}) + \left.\frac{\partial J_1}{\partial \phi_2}\right|_{\phi_1}^{k} (\phi_2 - \phi_{2k}) \tag{99}$$

and

$$J_2 = \hbar j_2 + \left.\frac{\partial J_2}{\partial \phi_1}\right|_{\phi_2}^{k} (\phi_1 - \phi_{1k}) + \left.\frac{\partial J_2}{\partial \phi_2}\right|_{\phi_1}^{k} (\phi_2 - \phi_{2k}) \tag{100}$$

around (ϕ_{1k}, ϕ_{2k}). Using the fact that $\left.\partial J_2/\partial \phi_1\right|_{\phi_2}$ is the opposite of $\left.\partial J_1/\partial \phi_2\right|_{\phi_1}$ [see Eqs. (62) and (76)], these developments lead to

$$\phi_1 = \phi_{1k} + \frac{\left.\partial J_2/\partial \phi_2\right|_{\phi_1}^{k} (J_1 - \hbar j_1) - \left.\partial J_1/\partial \phi_2\right|_{\phi_1}^{k} (J_2 - \hbar j_2)}{\left.\partial J_2/\partial \phi_2\right|_{\phi_1}^{k} \left.\partial J_1/\partial \phi_1\right|_{\phi_2}^{k} + \left(\left.\partial J_1/\partial \phi_2\right|_{\phi_1}^{k} \right)^2}. \tag{101}$$

By comparing the derivative of ϕ_1 with respect to J_2 at fixed J_1 and Eqs. (88) and (89), one recovers Eq. (98).

From Eqs. (81)–(85), Eq. (98) and the identity

$$\Omega + \pi_1 R_1 - \pi_2 R_2 + J_1 \phi_1 - J_2 \phi_2 = \bar{\Omega} = -\int_0^t d\tau (R\dot{P} + \phi \dot{J}) \tag{102}$$

obtained by integration by part, $S_{j_2 j_1}(E)$ takes the compact form

$$S_{j_2 j_1}(E) = g \sum_k \left(\frac{2\pi i}{\hbar} \left| \frac{\partial J_2}{\partial \phi_1} \right|_{J_1}^{k} \right| \right)^{-1/2} e^{i[\bar{\Omega}_k/\hbar - \pi \chi_k/2]} \tag{103}$$

which is the first key expression of the paper. Noting from Eq. (102) that

$$\phi_1 = \frac{\partial \bar{\Omega}}{\partial J_1}, \tag{104}$$

Eq. (103) can be rewritten as

$$S_{j_2 j_1}(E) = g \sum_k \left(\frac{\hbar}{2\pi i} \left| \frac{\partial^2 \bar{\Omega}}{\partial J_2 \partial J_1} \right|_k \right)^{1/2} e^{i[\bar{\Omega}_k/\hbar - \pi \chi_k/2]} \tag{105}$$

or from Eqs. (77) and (79),

$$S_{j_2 j_1}(E) = g \sum_k \left(\frac{1}{2\pi i \hbar} \left| \frac{\partial^2 \bar{\Omega}}{\partial j_2 \partial j_1} \right|_k \right)^{1/2} e^{i[\bar{\Omega}_k/\hbar - \pi \chi_k/2]}, \tag{106}$$

which reminds us of the Van Vleck–Gutzwiller space-time propagator in one dimension [55,56]. The reader interested in the general analysis of the semiclassical form of matrix elements is referred to the major work by Miller on correspondence relations [32]. We hope that considering j_2 and j_1 as an integer on the left-hand side of Eq. (106) and real on the right-hand side is not confusing. This expression is, however, only of formal interest, contrary to Eq. (103).

The sum in Eqs. (103) and (106) is recognized as the classic Miller-Marcus CSMT expression but the phase index χ_k has now a clear mathematical definition. In addition to that, a supplementary factor g has emerged from the developments. From Eqs. (19), (20), (78), and (80), it is, however, clear that the amplitude of this factor [see Eq. (82)] is significantly lower than one only when $|j_1|$ and/or $|j_2|$ are close to $j_{max} = (2IE)^{1/2}/\hbar$. As a consequence, keeping g at 1 (its phase is irrelevant) will be an excellent approximation provided that j_{max} is not too small [91].

In such a case, the link between CSMT and the purely classical description clearly appears as follows: from Eq. (103), the final probability $P_{j_2 j_1}(E) = |S_{j_2 j_1}(E)|^2$ of measuring the rotational quantum number j_2 turns out to be

$$P_{j_2 j_1}(E) = \sum_k \left(\frac{2\pi}{\hbar} \left| \frac{\partial J_2}{\partial \phi_1} \right|_{J_1}^{k} \right| \right)^{-1} \tag{107}$$

when discarding the interference terms. This expression supposes them to be quenched as is typically the case when the collision proceeds through a long-lived complex and resonances dominate the dynamics. The $\bar{\Omega}_k$'s and χ_k's are then randomly distributed, thus leading to Eq. (107). However, a still intriguing fact is that related expressions work quite well for direct processes like the reaction $\mathrm{O}(^3\mathrm{P}) + \mathrm{HCl} \rightarrow \mathrm{OH} + \mathrm{Cl}$ [75] which proceeds through a simple barrier and should thus not involve too many resonances.

Equation (107) is strictly equivalent to [72,73]

$$P_{j_2 j_1}(E) = \frac{1}{2\pi} \int_0^{2\pi} d\phi_1 \delta(J_2(\phi_1)/\hbar - j_2) \tag{108}$$

with J_2 rewritten as $J_2(\phi_1)$ for clarity's sake. It is indeed straightforward to go from Eq. (108) to Eq. (107) by using the standard theorem

$$\delta(f(\phi)) = \sum_k |f'(\phi_k)|^{-1} \delta(\phi - \phi_k), \tag{109}$$

where $f(\phi_k) = 0$ [92]. $P_{j_2 j_1}(E)$ is recognized to be the classical density of probability that the rotational action $J_2(\phi_1)/\hbar$, i.e., the classical equivalent of the rotational quantum number, is equal to j_2. $P_{j_2 j_1}(E)$ according to Eq. (108) is thus not a probability in the classical sense. However, Eq. (108) is the result of quantum mechanics within the SPA, valid in the limit where $\hbar$ tends to zero (as compared to $\hbar j_{max}$). In this limit, the sum over the integer j_2 and the integral with respect to the real j_2 are equal. $P_{j_2 j_1}(E)$ is therefore normalized to unity and the density of probability becomes a probability.

In practice, the Dirac distribution in Eq. (108) is replaced by a Gaussian function the width ϵ of which is sufficiently small to account for quantization, and sufficiently large to converge the results [71]. We then have

$$P_{j_2 j_1}(E) = \frac{1}{2\pi^{3/2}\epsilon} \int_0^{2\pi} d\phi_1 e^{-(J_2(\phi_1)/\hbar - j_2)^2/\epsilon^2} \tag{110}$$

which may be solved by Monte Carlo integration. ϵ is often kept at ~ 0.05 in the calculations [74–77]. We shall later use this Gaussian weighting (GW) procedure for the practical calculation of S matrix elements.

3. ν_k is null

Let us rewrite M_k, given by Eq. (87), as

$$M_k = \begin{pmatrix} m_{11} & m_{12} \\ m_{21} & m_{22} \end{pmatrix}. \tag{111}$$

The two eigenvalues λ_- and λ_+ of M_k are given by

$$2\lambda_{\pm} = m_{11} + m_{22} \pm \Delta^{1/2}, \tag{112}$$

where the discriminant Δ is given by

$$\Delta = (m_{11} + m_{22})^2 - 4 \det(M_k) = (m_{11} - m_{22})^2 + 4m_{12}^2. \tag{113}$$

The second identity comes from the fact that in the present case, m_{12} and m_{21} are equal [see Eq. (87)]. This identity shows that Δ is positive and therefore λ_- and λ_+ are real (this property is typical of symmetric matrices).

If $\det(M_k)$ is positive, it is clear from Eq. (112) and the left identity of Eq. (113) that the two eigenvalues have the sign of $m_{11} + m_{22}$. From Eq. (97), $\det(M_k)$ can be rewritten as

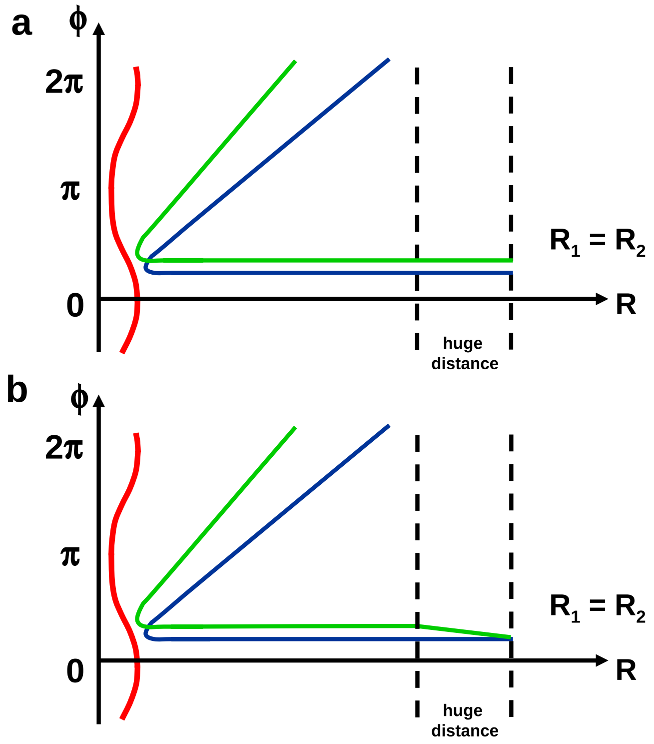

FIG. 5. (Color online) Examples of reflected paths with same initial conditions except a difference of $\delta\phi_1$ (a) and δJ_1 (b). See text for more details.

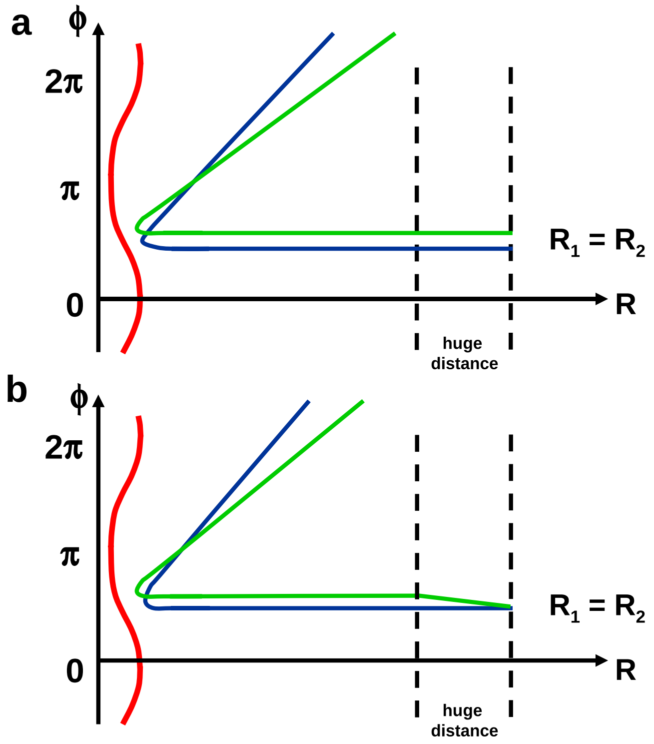

FIG. 6. (Color online) Same as Fig. 5.

$$\det(M_k) = \left.\frac{\partial J_2}{\partial \phi_1}\right|_{J_1}^{k} \Bigg/ \left.\frac{\partial \phi_2}{\partial J_1}\right|_{\phi_1}^{k} \tag{114}$$

while from Eqs. (87), (93), and (94), $m_{11}+m_{22}$ can be transformed to

$$m_{11}+m_{22} = \left(\left.\frac{\partial J_2}{\partial J_1}\right|_{\phi_1}^{k} + \left.\frac{\partial \phi_2}{\partial \phi_1}\right|_{J_1}^{k} \right) \Bigg/ \left.\frac{\partial \phi_2}{\partial J_1}\right|_{\phi_1}^{k} . \tag{115}$$

In Fig. 5, two paths coming from R_1 are scattered by a potential wall (this is not necessarily a hard wall). In panel (a), the blue path, labeled k, is defined by $J_1=0$ and a given value of ϕ_1 while the green path is defined by $J_1=0$ and $\phi_1+\delta\phi_1$ (with $\delta\phi_1$ positive). The wall being convex in the part seen by the trajectories, they eventually diverge in such a way that J_2 is larger for the green path than for the blue one. Consequently, both $\left|\partial J_2/\partial\phi_1\right|_{J_1}^{k}$ and $\left|\partial\phi_2/\partial\phi_1\right|_{J_1}^{k}$ are positive.

In the lower panel, the blue path is defined by $J_1=0$ and a given value of ϕ_1 while the green path is defined by δJ_1 (positive) and ϕ_1. Since the distance between the two vertical dashed lines is huge and δJ_1 is infinitesimal, the two paths are (almost) parallel when touching the wall. For the same reason as in Fig. 5(a), they eventually diverge in such a way that both $\partial J_2/\partial J_1|_{\phi_1}^{k}$ and $\partial\phi_2/\partial J_1|_{\phi_1}^{k}$ are positive.

In Fig. 6, the paths rebound against a concave part of the wall and J_2 is now lower for the green paths than for the blue ones. The four previous partial derivatives are thus negative. That these quantities have the same sign will be numerically illustrated in Sec. VIII.

From Eqs. (114) and (115), both $\det(M_k)$ and $m_{11}+m_{22}$ turn out to be positive, and so are λ_- and λ_+. Since ν_k is defined as the number of negative eigenvalues of M_k, ν_k is null.

Last but not least, it can be easily verified that modifying the conventions regarding the signs of $\delta\phi_1$ and δJ_1 or considering a topologically more complex interaction does not change the final result.

As a conclusion, *the phase index* χ_k *of classical S matrix elements is equal to the Maslov index* η_k *of the classical configuration space Green function.*

IV. 1D SCIVR TREATMENT

We now consider the 1D SCIVR description of $S_{j_2 j_1}(E)$ which goes beyond CSMT as far as the accuracy of the predictions are concerned.

Just as for CSMT, the starting point of this description is the set of Eqs. (67)–(69). However, instead of integrating over both ϕ_2 and ϕ_1 within the SPA, we shall only integrate over ϕ_1.

For the function f of a single variable x and s a sufficiently small parameter, the SPA states that

$$\int dx e^{if(x)/s} \approx \sum_k \left(\frac{2\pi i s}{|f_k''|} \right)^{1/2} e^{i(f_k/s-\pi n_k/2)}, \tag{116}$$

where x_k is the kth stationary point of f, $f_k=f(x_k)$, $f_k''=f''(x_k)$, and n_k is 0 if f_k'' is positive, 1 in the contrary case [54–56].

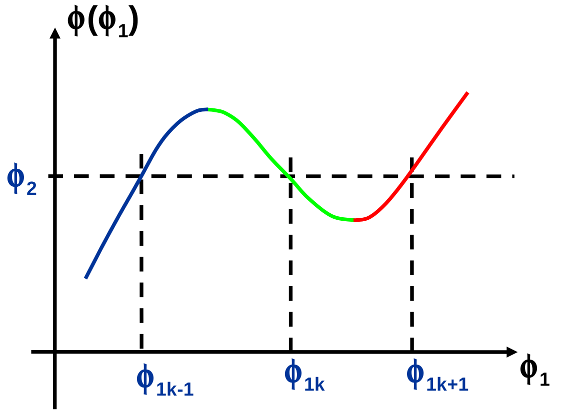

FIG. 7. (Color online) Schematic representation of ϕ in R_2 as a function of ϕ_1. Different colors (or grey intensities) correspond to different branches. Three of them are represented here.

In Eqs. (67)–(69), the small parameter s is again $\hbar$ and regarding the application of the SPA, the relevant part of the phase is now

$$f(\phi_1) = \Omega + \hbar j_1 \phi_1. \tag{117}$$

The stationary phase condition defines the values ϕ_{1k}'s of ϕ_1 contributing to $S_{j_2 j_1}(E)$ through

$$\hbar j_1 = - \left.\frac{\partial \Omega}{\partial \phi_1}\right|_{\phi_2} (\phi_2, \phi_{1k}). \tag{118}$$

This relation, together with Eq. (62), imply that J_1 is given by Eq. (77). Hence R_1, ϕ_{1k}, J_1 and P_1, given by Eq. (78), are the initial conditions of the classical paths reaching the configuration space point (R_2, ϕ_2) after visiting the interaction region.

For a given R_1 and the values of J_1 and P_1 mentioned above, the value of ϕ in R_2 is a function of ϕ_1, denoted $\phi(\phi_1)$. A plausible shape is represented in Fig. 7. The values ϕ_{1k} leading to $\phi(\phi_1)$ equal ϕ_2 are shown. In each branch k, ϕ_{1k} can be seen as a function of ϕ_2. A sum over these branches of a given integral over ϕ_2 can thus be transformed in a single integral over ϕ_1. This is the IVR trick, initially introduced by Miller [21]. The terminology *initial value representation* comes from the fact that the resulting integrand is now depending on the quadruplet (R_1, ϕ_1, P_1, J_1) of initial conditions.

Integrating over ϕ_1 in Eq. (67) within the SPA precisely leads to a sum over k of integrals over ϕ_2. Using the IVR trick, the previous quantity can thus be expressed as a simple integral over ϕ_1. The integrand involves the term $\partial^2\Omega/\partial\phi_1^2|_{\phi_2}$, i.e., the opposite of $\partial J_1/\partial\phi_1|_{\phi_2}$ [see Eq. (62)]. The latter satisfies Eq. (93), used to simplify the integrand. The manipulations pose no difficulty and lead to the second key expression of the paper:

$$S_{j_2 j_1}(E) = \frac{1}{2\pi i}\int_0^{2\pi} d\phi_1 \left| \left.\frac{\Pi_1 \Pi_2}{\pi_1 P_2}\frac{\partial \phi_2}{\partial \phi_1}\right|_{J_1} \right|^{1/2} e^{i[\Phi/\hbar - \pi(\eta+n)/2]} \tag{119}$$

with

$$\Phi = (\Pi_1 - \pi_1)R_1 + (P_2 - \Pi_2)R_2 + (J_2 - \hbar j_2)\phi_2 + \bar{\Omega}. \tag{120}$$

In the above expressions, P_2, ϕ_2, η, n, J_2 and $\bar{\Omega}$ are implicit functions of ϕ_1.

n is zero if $\partial^2\Omega/\partial\phi_1^2|_{\phi_2}$ is positive, i.e., if $\partial J_1/\partial\phi_1|_{\phi_2}$ is negative. From Eq. (93), this amounts to stating that n is zero if $\partial\phi_2/\partial\phi_1|_{J_1}$ and $\partial\phi_2/\partial J_1|_{\phi_1}$ have the same sign. Following the reasoning of the previous section based on Figs. 5 and 6, this is just the conclusion we arrive at. As a matter of fact, the phase index reduces to η, as in CSMT.

Since in most cases, Π_1 and π_1 are very close, we can rewrite $S_{j_2 j_1}(E)$ as

$$S_{j_2 j_1}(E) = \frac{1}{2\pi i}\int_0^{2\pi} d\phi_1 \left| \left.\frac{\pi_2}{P_2}\frac{\partial \phi_2}{\partial \phi_1}\right|_{J_1} \right|^{1/2} e^{i(\Phi/\hbar - \pi\eta/2)} \tag{121}$$

with

$$\Phi = (P_2 - \pi_2)R_2 + (J_2 - \hbar j_2)\phi_2 + \bar{\Omega}. \tag{122}$$

This expression bears some common features with Miller's one [see Eq. 29 in [21]] and is in even closer agreement with an expression derived by Connor and Marcus [see Eqs. (2.5) and (2.6) in [36]]. However, the phase index is now clearly specified.

V. 2D SCIVR TREATMENT

The starting point is still the set of Eqs. (67)–(69) but instead of applying the SPA, one replaces the integration variable ϕ_2 by J_1 which, together with R_1, ϕ_1, and Eq. (92), determine the initial conditions of the trajectory. Consequently, the sum over trajectories in Eq. (69) disappears. Using the fact that $\partial^2\Omega/\partial\phi_2\partial\phi_1$ is equal to the opposite of $\partial J_1/\partial\phi_2|_{\phi_1}$ [see Eq. (62)], we arrive after a few steps of algebra at the third key expression of the work, i.e.,

$$S_{j_2 j_1}(E) = \int d\phi_1 dJ_1 q(\phi_1, J_1) u(\phi_1, J_1) \tag{123}$$

with

$$q(\phi_1, J_1) = \frac{1}{(2\pi i\hbar)^{1/2}}\frac{1}{2\pi i} e^{i(\Pi_1 R_1 - \Pi_2 R_2 + \hbar j_1 \phi_1 - \hbar j_2 \phi_2)/\hbar} \tag{124}$$

and

$$u(\phi_1, J_1) = \left| \left.\frac{\Pi_1 \Pi_2}{P_1 P_2}\frac{\partial \phi_2}{\partial J_1}\right|_{\phi_1} \right|^{1/2} e^{i(\Omega/\hbar - \pi\eta/2)}. \tag{125}$$

In the above expressions, P_1, P_2, ϕ_2, Ω, and η are implicit functions of both ϕ_1 and J_1. The phase index is again η.

VI. 3D SCIVR TREATMENT

We turn back to the initial Eqs. (17) and (18). By using the closure relation (28), we arrive at

$$S_{j_2j_1}(E) = \frac{a}{2\pi}\int dt d\phi_2 d\phi_1 v(t,\phi_2,\phi_1) \tag{126}$$

with

$$v(t,\phi_2,\phi_1) = e^{iEt/\hbar}e^{i(j_1\phi_1 - j_2\phi_2)}\langle R_2\phi_2|e^{-i\hat{H}t/\hbar}|R_1\phi_1\rangle. \tag{127}$$

The Van Vleck–Gutzwiller semiclassical approximation of the space-time propagator is [54–56,63]

$$\langle R_2\phi_2|e^{-i\hat{H}t/\hbar}|R_1\phi_1\rangle_{sc} = \sum_{Traj}\frac{|\Delta|^{1/2}}{2\pi i\hbar}e^{i(W/\hbar - \pi\kappa/2)}, \tag{128}$$

where

$$\Delta = \det(M_t), \tag{129}$$

$$M_t = \begin{pmatrix} -\dfrac{\partial^2 W}{\partial R_t \partial R_1} & -\dfrac{\partial^2 W}{\partial R_t \partial \phi_1} \\ -\dfrac{\partial^2 W}{\partial \phi_t \partial R_1} & -\dfrac{\partial^2 W}{\partial \phi_t \partial \phi_1} \end{pmatrix}, \tag{130}$$

$$W = \int_0^t d\tau L, \tag{131}$$

and the index κ is the sum of the numbers of time each eigenvalue of M_τ^{-1} changes sign when τ runs from 0 to t. Note that within the above notations, $R_\tau = R_1$ and $\phi_\tau = \phi_1$ when $\tau = 0$ while $R_\tau = R_2$ and $\phi_\tau = \phi_2$ when $\tau = t$.

From the identities $P_1 = -\partial W/\partial R_1|_{R_2}$ and $J_1 = -\partial W/\partial \phi_1|_{\phi_2}$, deduced from Eqs. (3), (6), (8), and (131), we arrive at

$$\Delta^{-1} = \det(M_t^{-1}) = \begin{vmatrix} \dfrac{\partial R_2}{\partial P_1} & \dfrac{\partial R_2}{\partial J_1} \\ \dfrac{\partial \phi_2}{\partial P_1} & \dfrac{\partial \phi_2}{\partial J_1} \end{vmatrix}. \tag{132}$$

We now follow the approach by Skinner and Miller [64,65]. Including the right-hand side of the identity

$$1 = \int dR_t \delta(R_t - R_2) \tag{133}$$

in the integrand of Eq. (126), accounting for Eq. (128) and integrating over t using theorem (109) leads to

$$S_{j_2j_1}(E) = \frac{a}{4\pi^2 i\hbar}\sum_{Traj}\int dR_2 d\phi_2 d\phi_1 w(R_2,\phi_2,\phi_1) \tag{134}$$

with

$$w(R_2,\phi_2,\phi_1) = \frac{|\Delta|^{1/2}}{|\dot{R}_2|}e^{i[(Et+W)/\hbar + j_1\phi_1 - j_2\phi_2 - \pi\kappa/2]}. \tag{135}$$

We now replace the integration variables R_2 and ϕ_2 by P_1 and J_1, which, together with R_1 and ϕ_1, determine the initial conditions of the trajectory. For similar reasons as in sec. IV, the sum over trajectories in Eq. (134) disappears. Noting that

$$dR_2 d\phi_2 = |\Delta^{-1}| dP_1 dJ_1 \tag{136}$$

with Δ^{-1} given by Eq. (132), we finally arrive at the fourth key expression of the paper, i.e.,

$$S_{j_2j_1}(E) = \frac{\mu a}{4\pi^2 i\hbar}\int dP_1 dJ_1 d\phi_1 y(P_1,J_1,\phi_1) \tag{137}$$

with

$$y(P_1,J_1,\phi_1) = \frac{|\Delta^{-1}|^{1/2}}{P_2}e^{i[(Et+W)/\hbar + j_1\phi_1 - j_2\phi_2 - \pi\kappa/2]}. \tag{138}$$

In the above expression, Δ^{-1}, P_2, W, t, ϕ_2, and κ are implicit functions of P_1, J_1, and ϕ_1.

VII. EXACT QUANTUM SCATTERING CALCULATIONS

The quantum scattering calculations have been performed by using a time-dependent method based on the multiconfiguration time-dependent Hartree (MCTDH) propagation scheme [93–96]. Only the key features of the MCTDH method will be exposed here, all the details of it being reviewed in the previous references.

The wave function describing the time-evolution of a f-dimensional system is expanded in a basis of time-dependent wave functions, called single particle functions (SPFs), as follows:

$$\begin{aligned}\Psi(Q_1,\ldots,Q_f,t) &= \sum_{j_1=1}^{n_1}\cdots\sum_{j_f=1}^{n_f}A_{j_1\cdots j_f}(t)\prod_{\kappa=1}^{f}\varphi_{j_\kappa}^{(\kappa)}(Q_\kappa,t) \\ &= \sum_J A_J\Phi_J. \end{aligned}\tag{139}$$

The Q_k's denote the f configuration space coordinates, $A_{j_1\cdots j_f}$ the expansion coefficients, and $\varphi_{j_\kappa}^{(\kappa)}$ the SPF for each degree of freedom [97]. These SPFs are in turn expanded in a regular time-independent basis set $\chi_{i_\kappa}^{(\kappa)}(Q_\kappa)$:

$$\varphi_{j_\kappa}^{(\kappa)}(Q_\kappa,t) = \sum_{i_\kappa=1}^{N_\kappa}c_{i_\kappa j_\kappa}^{(\kappa)}(t)\chi_{i_\kappa}^{(\kappa)}(Q_\kappa). \tag{140}$$

The $\chi_{i_\kappa}^{(\kappa)}(Q_\kappa)$ are usually chosen as the basis functions of a discrete variable representation (DVR) and the size of the SPF expansion in Eq. (140) is determined by the phase space spanned by the system for the degree of freedom κ. It is important to note that the SPFs are one-dimensional basis functions, so that the wave function is described by an expansion in Hartree products, each of the Hartree products representing a configuration within a multiconfigurational scheme. As a consequence, the correlation between the various degrees of freedom is represented by the multiconfigurational nature of Eq. (139). The correct description of the correlation between the degrees of freedom converges with the number of SPFs (number of configurations). A balance has to be found between the correct description of the correlation and the computational time which increases with the number of SPFs.

The equation of motion for the expansion coefficients and the SPFs are derived from the Dirac-Frenkel variational principle $\langle \delta\Psi | \hat{H} - i\frac{\partial}{\partial t} | \Psi \rangle = 0$ leading to a set of coupled equations which requires less computational effort than standard methods for high-dimensional problems. The reason is that the wave function can often be expanded in a much lower number of SPFs, n_κ, than the number of basis functions, N_κ, used in standard wave-packet propagation schemes. By increasing the number of SPFs one can obtain a more and more accurate determination of the dynamical quantities and the wave function converges to the exact solution (the MCTDH method naturally converges to standard methods for $n_\kappa = N_\kappa$).

To summarize, the MCTDH method is a quantum wave-packet propagation scheme based on wave functions expanded in a reduced basis set (SPFs) variationally optimized in time, in order to keep the size of the problem as small as possible. In practice, the interest of using SPFs is a reduction of the amount of memory required to store the wave function as well as a reduction of the computational time used for the propagation.

Molecular scattering can be described within MCTDH by propagating a wave packet initially located in the reagents up to the products where it is finally analyzed.

As far as our model system is concerned, the initial wave-packet function is given by

$$\Psi(R,\phi;t=0) = G_0(R)\varphi_1(\phi). \tag{141}$$

$G_0(R)$ is a Gaussian wave-packet defined as

$$G_0(R) = (\sqrt{2\pi}\sigma)^{-1/2} \exp\left[-\left(\frac{R-R_1}{2\sigma}\right)^2\right] \exp[-iP_0(R-R_1)]. \tag{142}$$

The width σ, the initial momentum P_0, and the initial position R_1 are the parameters defining the initial wave packet. These values are respectively kept at 0.8, −6.7 and 10 in atomic unit.

$\varphi_1(\phi)$, given by Eq. (15), is the wave function corresponding to the rotational state $|j_1\rangle$.

The SPFs used to describe the wave function are represented by different DVR and/or fast fourier transform (FFT) representations.

The quantum Hamiltonian is given by

$$\hat{H} = -\frac{\hbar^2}{2\mu}\Delta_R - \frac{\hbar^2}{2I}\Delta_\phi + V, \tag{143}$$

where Δ_R and Δ_ϕ are the Laplacians associated with R and ϕ.

The state-selected scattering probabilities are computed with the help of a complex adsorbing potential (CAP) located in the asymptotic region defined by R larger than $R_{as} = 15$ a.u., combined with a flux analysis procedure [98]. The CAP used to adsorb the scattered back wave packet is a one-dimensional potential function of the following form:

$$iW_R(R) = i\gamma |R - R_{as}|^\rho \Theta(R - R_{as}). \tag{144}$$

The parameters R_{as}, γ, and ρ respectively define the starting point, strength, and order of the CAP. γ is kept at 0.0029 and ρ at 2. Θ is the Heaviside step function.

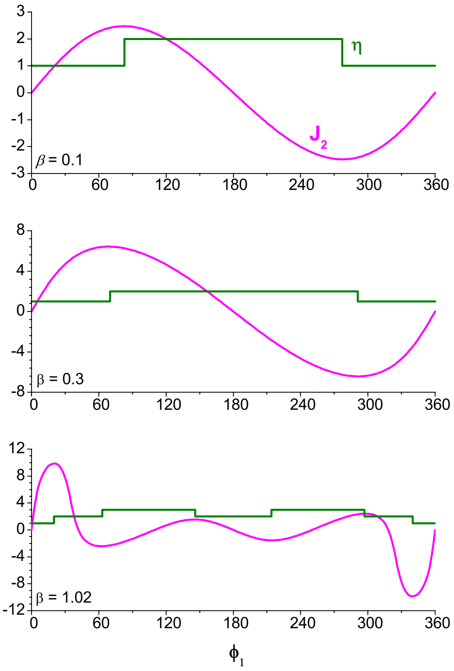

FIG. 8. (Color online) Collisional function (magenta curves) and the Maslov index η (green steps) for the interaction potential (145) (see text for the values of the mechanical parameters used in the calculations). The three panels correspond to β equal 0.1 (upper panel), 0.3 (middle panel), and 1.02 Å (lower panel), respectively.

VIII. COMPARISON BETWEEN CSMT, SCIVR, AND EQS RESULTS

CSMT and the three previously derived SCIVR approaches are now applied to the atom rigid rotor collision governed by the potential

$$V = e^{-\alpha(R-\beta\cos\phi)}. \tag{145}$$

While α is kept at 2 Å^{-1}, β is kept at the three different values 0.1, 0.3, and 1.02 Å corresponding to increasing couplings between the R and ϕ coordinates in the interaction region. j_1 is zero, E is equal to 0.5 eV, μ is kept at 2/3 amu, m at 1/2 amu, and r is equal to 1 Å. These parameters lead to strong quantum interferences, as shown further below.

The collision function, i.e., the final value $J_2 \equiv J_2(\phi_1)$ of J in terms of the initial angle ϕ_1, is represented in Fig. 8, together with the phase index η. R_1 and R_2 were both kept at 200 Å (as explained further below, such large values are unnecessary for getting accurate transition probabilities), and Eqs. (77) and (78) define the rest of the initial conditions. The collision function involves smooth oscillations and the phase index increases or decreases by one unit at each extremum of the former. Both quantities are symmetric with respect to π, as expected from the form of V.

Quantities proportional to the four partial derivatives of Sec. III B 3 are represented in Fig. 9 for β kept at 0.1. These quantities are in fact the partial derivatives divided by their absolute values in ϕ_1 equal to zero, and multiplied by 1 [$\partial J_2/\partial\phi_1|^k_{J_1}$, red curve (curve starting at 1)], 2 [$\partial\phi_2/\partial\phi_1|^k_{J_1}$, green curve (curve starting at 2)], 3 [$\partial J_2/\partial J_1|^k_{\phi_1}$, blue curve

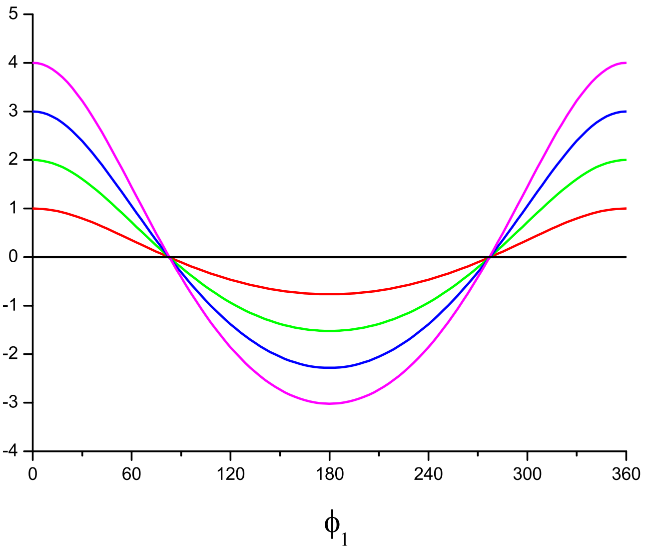

FIG. 9. (Color online) Quantities proportional to the four partial derivatives $\partial J_2/\partial\phi_1|_{J_1}^k$ [red curve (curve starting at 1)], $\partial\phi_2/\partial\phi_1|_{J_1}^k$ [green curve (curve starting at 2)], $\partial J_2/\partial J_1|_{\phi_1}^k$ [blue curve (curve starting at 3)], and $\partial\phi_2/\partial J_1|_{\phi_1}^k$ [magenta curve (curve starting at 4)] in terms of ϕ_1. β is kept at 0.1. See text for more details.

(curve starting at 3)], and 4 [$\partial\phi_2/\partial J_1|_{\phi_1}^k$, magenta curve (curve starting at 4)]. Since the four derivatives have quite different values, the previous rescaling was necessary to represent their shapes in the same graphic while being still able to distinguishing them. As a matter of fact, the four derivatives turn out to have the same sign, in agreement with the conclusions of the reasoning developed in Sec. III B 3.

The β values were chosen in such a way that J_2 is not too close to an integer at the extrema. We know from Sec. III B 2 that the classical paths mainly contributing to S matrix elements are those satisfying the boundary conditions (77) and (79), i.e., connecting integer actions of the reagents and integer actions of the products. There will therefore be no value of k in Eq. (103) for which $\partial J_2/\partial\phi_1|_{J_1}^k$ tends to zero. In other words, the probability amplitudes carried by the previous paths will not tend to infinity. This is a prerequisite for avoiding any rainbow effect in CSMT predictions [32,49,50].

We intentionally considered a system not involving any resonance, or equivalently, trapped trajectory, for it is well known that up to the present, semi-classical approaches have failed at reproducing EQS results when resonances dominate the dynamics [24,61]. The basic reason is that the collision function has a fractal structure in resonance regions [24,99]. Therefore Eq. (79) has an uncountable number of roots for which $\partial J_2/\partial\phi_1|_{J_1}^k$ tends to infinity. The problem is thus numerically intractable. As far as SCIVR approaches are concerned [see Eqs. (121), (123), (125), (137), and (138)], the problem is similar as the amplitude factor of the integrand diverges for trapped trajectories. As most realistic systems involve strong resonances, building a method circumventing the resonance problem is a major challenge of semiclassical collision theory.

Extrema of J_2 correspond in fact to focal points at infinity. In other words, if the reference path of Sec. III A 3 corresponds to an extremum of J_2, its neighboring trajectories will cross it at infinity. Considering the case where η gains one unit at a given value ϕ_1^g of ϕ_1 when increasing the latter, the crossing, or focal, or conjugate point will first appear at infinity for ϕ_1^g exactly and then move inward when keeping ϕ_1 increasing. On the contrary, a decrease of η by one unit corresponds to a focal point disappearing at infinity.

We have found it necessary to keep R_1 and R_2 at very large values (more than ~100 Å) to find a close correspondence between extrema of the collision function and jumps of the phase index. However, predicting accurate values of η in the neighborhood of the extrema is not a necessary condition to obtain accurate rotational state distributions in the cases considered; as stated above, the extrema do not correspond to integer values of J_2 and therefore, according to CSMT, trajectories associated with these extrema do not significantly contribute to S matrix elements. There is thus no need to accurately know η around the extrema and therefore to take R_1 and R_2 at very large values when calculating S matrix elements.

As far as CSMT is concerned, the classical paths contributing to $S_{j_2j_1}(E)$ are usually determined either by graphically solving Eq. (79) or by building a root-search algorithm. $S_{j_2j_1}(E)$ is then calculated from Eq. (103) (for simplicity's sake, we keep the g factor at 1, an excellent approximation in the cases presently considered). However, we have found it quite convenient to rewrite Eq. (103) as

$$S_{j_2j_1}(E)=\int_0^{2\pi}d\phi_1\left(\frac{\hbar}{2\pi i}\left|\left.\frac{\partial J_2}{\partial\phi_1}\right|_{J_1}\right|\right)^{1/2}\times\delta(J_2(\phi_1)-\hbar j_2)e^{i[\bar{\Omega}/\hbar-\pi\eta/2]} \tag{146}$$

[it is indeed an easy task to prove this result using Eq. (109)] and replace the Dirac distribution by a numerically friendly Gaussian function leading to

$$S_{j_2j_1}(E)=\int_0^{2\pi}d\phi_1\left(\frac{\hbar}{2i}\left|\left.\frac{\partial J_2}{\partial\phi_1}\right|_{J_1}\right|\right)^{1/2}\frac{1}{\pi\epsilon}\times e^{-[J_2(\phi_1)-\hbar j_2]^2/\epsilon^2}e^{i[\bar{\Omega}/\hbar-\pi\eta/2]}. \tag{147}$$

CSMT is thereby transformed to a SCIVR method going around the root-search problem. We note that in the case of resonances, Eq. (147) also suffers from the divergence of the integrand amplitude for trapped trajectories. On the other hand, a great advantage of the GW-QCT method [see Eq. (110)] is that it is divergence free.

CSMT results are totally independent of the values of R_1 and R_2 provided that they are larger than ~5 Å, the distance beyond which V can be considered as zero. On the other hand, SCIVR results depend significantly on R_1 and R_2 (even when these are larger than ~5 Å). The reason is that the phases in the integrands of Eqs. (121), (123), and (137) depend strongly on the previous distances. Therefore the contribution of each trajectory to $S_{j_2j_1}(E)$ evolves in terms of R_1 and R_2. If an infinite number of trajectories could be run, the total sum of their contributions would not depend on R_1 and R_2, but this will not be so if this number is finite (as is necessarily the case). For the present study, we run between

~1000 (1D SCIVR) and ~50 000 (3D SCIVR) trajectories. In addition to that, the 2D and 3D SCIVR results also depend on the boundaries of integration along the J_1 axis (2D approach), and in the (P_1, J_1) plane (3D approach). We then found it reasonable to retain those values of R_1, R_2 and the previous boundaries which better comply with the unitarity of the S matrix, and finally re-normalized the populations to make their sum equal to 1 exactly.

These quantities are shown in Fig. 10 (magenta and blue curves), together with the EQS predictions (green curves). As previously stated, they show strong interference patterns. The good to close agreement found between semiclassical expectations and exact quantum results is pleasing (we also used Filinov filtering [65,100–102], but this procedure did not seem to improve the results). We note the quantitative jump when going from CSMT to the 1D-SCIVR treatment while the improvement of the results when going from the latter to the 3D-SCIVR treatment is necessarily more moderate; 1D-SCIVR results are already very satisfying, which is quite encouraging as far as multidimensional processes are concerned. It is fascinating that classical mechanics plus the superposition principle lead to such a level of description of quantum interferences, especially when they are so strong.

For β equal to 0.1 and 0.3, the collision function is a simple sinusoid (see Fig. 8) and Eq. (79) has only two roots. This situation reminds us of the much studied vibrationally inelastic collision on the Secrest-Johnson potential energy surface (PES) [21]. The Maslov index η is one unit larger when J_2 decreases than when J_2 increases (see Fig. 8). It is a simple matter to show that in such a case, $P_{j_2 j_1}(E)$ reads

$$P_{j_2 j_1}(E) = p_1 + p_2 + 2(p_1 p_2)^{1/2} \sin[(\bar{\Omega}_2 - \bar{\Omega}_1)/\hbar], \tag{148}$$

where

$$p_k = \left(\frac{2\pi i}{\hbar} \left| \frac{\partial J_2}{\partial \phi_1} \right|_{J_1}^{k} \right)^{-1}, \tag{149}$$

$k=1,2$, is the (density of) probability carried by the kth trajectory [21,32,49,50]. The first and second roots correspond to J_2 increasing and decreasing, respectively. This amounts to taking the Maslov index at 0 when J_2 increases and 1 in the contrary case. p_1+p_2 is the classical population [see Eq. (107)] while the sinus term represents the quantum interference. This expression allows us to nicely interpret the differences between the classical and quantum mechanical predictions.

For β equal to 1.02, there are either two or four or six roots. In the two roots case, Eq. (148) is still valid. In the four and six roots cases, the expressions of $P_{j_2 j_1}(E)$ are more complex and not considered here.

One might think, from previous works [32,49,50], that taking η at 0 when J_2 increases and 1 in the contrary case is a general rule. However, the lower panel of Fig. 8 shows that η takes successively the values 1, 2, 3, 2, 3, 2, 1, or equivalently, 0, 1, 2, 1, 2, 1, 0. The previous rule is therefore only valid in the two roots case. In the four and six roots cases, applying it leads to results in complete disagreement with EQS results. In general, η should be calculated according to the method of Sec. III A 3 or any alternative one.

IX. REMARKS ON THE APPLICATION OF CSMT TO VIBRATIONALLY INELASTIC AND REACTIVE PROCESSES

Let us consider a collinear inelastic atom-diatom collision. The usual Jacobi coordinates (R, r) are considered as well as their conjugate momenta (P, p). The difference with the previous system is that ϕ is now fixed at zero while r is allowed to vary. An alternative to r and p are the angle-action coordinates q and n [32,49,50]. q is the vibrational phase of the diatom and n is its vibrational action. The initial and final vibrational quantum numbers are denoted n_1 and n_2, respectively. By using different approaches, Miller and Marcus showed that the S matrix element $S_{n_2 n_1}(E)$ is given by

$$S_{n_2 n_1}(E) = \sum_k \left(2\pi i \left| \frac{\partial n_2}{\partial q_1} \right|_{n_1}^{k} \right)^{-1/2} e^{i[\bar{\Omega}_k - \pi\eta_k/2]} \tag{150}$$

with $\bar{\Omega}_k$ equal to

$$\bar{\Omega} = -\int_0^t d\tau (R\dot{P} + q\dot{n}) \tag{151}$$

for the kth trajectory [20,34]. Actions are expressed in $\hbar$ unit and times 0 and t correspond to R equal to the large values R_1 and R_2, respectively. In the same spirit as for rotational transitions, the classical paths contributing to the sum are those starting with n equal to n_1 and ending with n equal to n_2.

Miller arrived at the above result by showing the close link between generating functions in classical mechanics and unitary transformations in quantum mechanics [20,32]. Later, he gave a second derivation of the above expression which starting point is the formal equivalent of Eq. (17) for vibrationally inelastic collisions. Our approach was of course mainly inspired by his second derivation. Marcus arrived at about the same conclusions by a WKB type approach [34]. However, the phase index was not initially present in these approaches, and we added it in Eq. (150).

In order to justify this index from first principles, we tried to extend the developments of Sec. III to the present situation, without success, however. The basic reason is that the previous developments involve the semiclassical Green function (36) in the (R, ϕ) plane, the equivalent of which would be the semi-classical Green function in the (R, q) plane. The problem is that the latter might be meaningless, as defining coordinates parallel and perpendicular to a given classical path in the (R, q) plane is quite problematic. R and q can hardly be mixed. This is actually the reason why we chose an atom-rigid rotor collision for our study of the phase index problem.

In the case of the Secrest-Johnson PES, the collision function is a simple sinusoid leading to two roots. We thus applied the analogs of Eqs. (148) and (149) with the same convention as previously, i.e., the first and second roots correspond to n_2 increasing and decreasing, respectively. How-

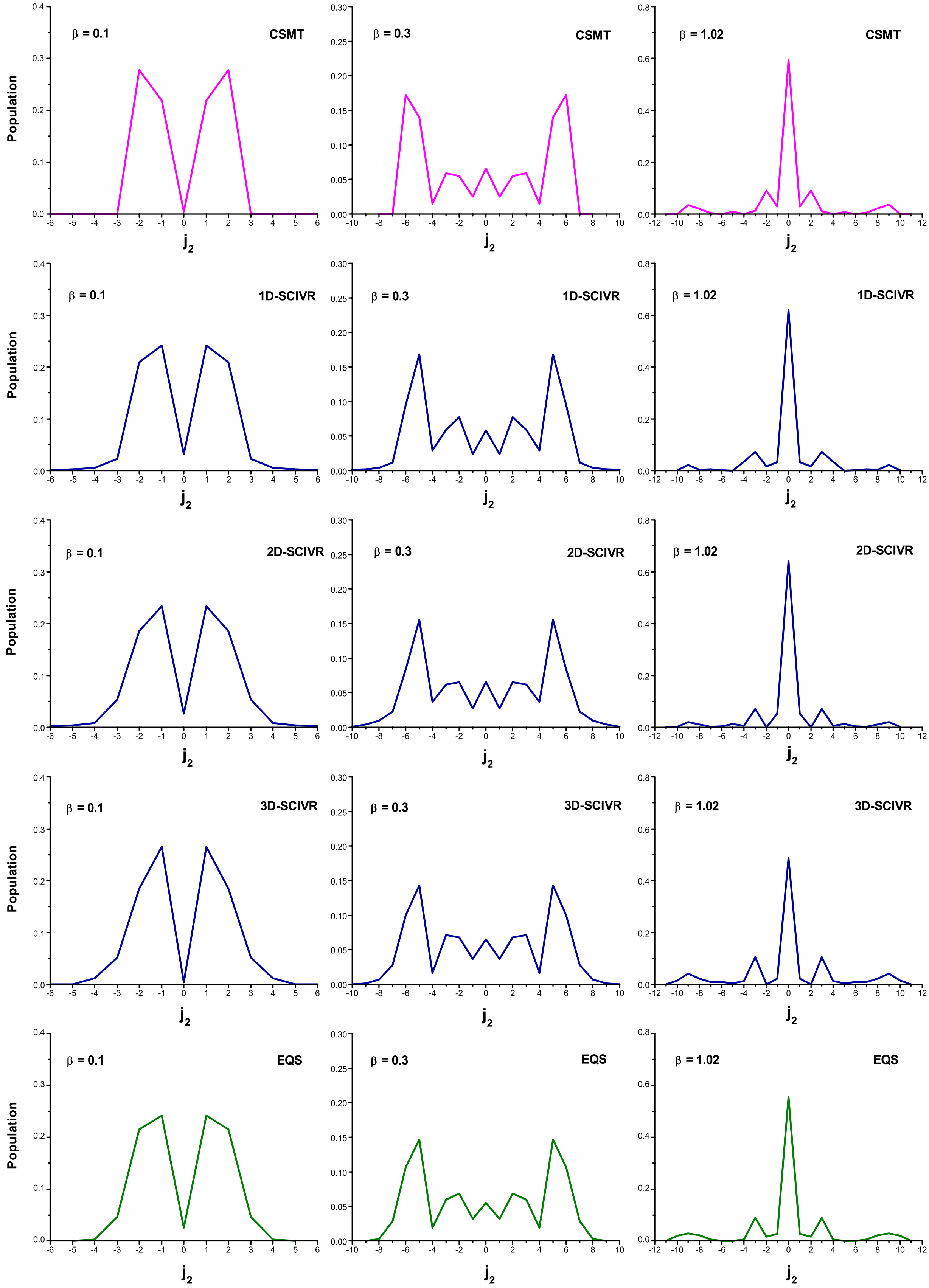

FIG. 10. (Color online) Rotational state distributions found from CSMT (magenta curves), three SCIVR treatments (blue curves), and EQS (green curves) calculations for the interaction potential (145) (see text for the values of the mechanical parameters used in the calculations).

ever, we only recovered part of the populations of Ref. [21]. On the other hand, the remaining populations were recovered when using the opposite convention. But in doing that, the previously correct populations turned out to be wrong. It seems therefore that if the magnitudes of interference terms are correctly described by this approach, their signs remain uncertain.

An alternative approach suggested by Stine and Marcus [47] and used later by van de Sand and Rost [60] is as follows: $S_{n_2n_1}(E)$ is still given by Eq. (150) with $\bar{\Omega}_k$ equal to

$$\bar{\Omega} = -\int_0^t d\tau (R\dot{P} + r\dot{p}) \qquad (152)$$

or

$$\bar{\Omega} = -\int_0^t d\tau (R\dot{P} - p\dot{r}) \qquad (153)$$

for the kth trajectory. Moreover, trajectories are started at an inner turning point. The first trajectory is, for instance, started at R_1, and the last one at $R_1 + \Delta R$ with ΔR such that the two previous trajectories are in fact the same. Trajectories are also stopped at an inner turning point in the final channel. The Maslov index η is then calculated in the (R, r) plane using, for instance, a method similar to the one of Sec. III A 3. We applied this method to the Secrest-Johnson PES using the Gaussian weighting procedure and this time, all the populations were found to be in close agreement with those of Ref. [21]. In addition to that, the method can be used as such for reactive collisions [47].

However, for the present time, we are not aware of any real justification of the method from first principle.

X. CONCLUSION

Semiclassical approaches of molecular collisions pioneered by Miller and Marcus in the early 1970s need phase indices, related to focal and turning points along trajectories contributing to S matrix elements. These indices are crucial for accurate descriptions of quantum interferences.

The main purpose of the work was to revisit the previous approaches in the case of a two degrees of freedom rotationally inelastic collision so as to make phase indices explicitly appear from first principles.

Classical S matrix theory (CSMT) and three semiclassical initial value representation (SCIVR) treatments, respectively involving simple, double, and triple integrals, were considered. The phase index is either the Maslov index of the classical configuration space Green function (CSMT and the first two SCIVR methods), or the Maslov index of the Van Vleck–Gutzwiller space-time propagator (third SCIVR method).

The validity of the four previous approaches was checked by comparing their predictions with exact quantum scattering results for interaction potentials leading to strong quantum interferences. There is a net improvement of the predictions when going from CSMT to the 1D-SCIVR treatment while the improvement is more moderate when going from the 1D to 3D-SCIVR treatment. The fact that 1D-SCIVR results are already very satisfying is quite encouraging as far as multidimensional processes are concerned.

The Gaussian weighting procedure, limited to the quasiclassical trajectory method up to now, was used in this work for practical CSMT calculations.

Standard applications of CSMT were finally discussed in the light of the previous developments and results.

The interaction potentials considered in this work do not lead to resonances. Extending the applicability of the previously discussed approaches to situations where resonances play a non-negligible role is a challenge of molecular collision theory.

ACKNOWLEDGMENTS

I wish to thank Professor J.-C. Rayez for stimulating discussions on the content of the present paper, and M. L. González-Martinez and J. Rubayo-Soneira for helpful advice. The quantum dynamics calculations were performed with the Heidelberg MCTDH package [103].

[1] R. D. Levine, *Molecular Reaction Dynamics* (Cambridge University Press, Cambridge, England, 2005).

[2] I. N. Levine, *Quantum Chemistry*, 6th Ed. (Prentice-Hall, Englewood Cliffs, NJ, 2008).

[3] F. L. Pilar, *Elementary Quantum Chemistry*, Second Ed. (Dover Publications, New York, 2001).

[4] T. Helgaker, P. Jorgensen, and J. Olsen, *Molecular Electronic Structure Theory* (Wiley, New York, 2000).

[5] In the present work, we will be only concerned with electronically adiabatic molecular collisions.

[6] P. Honvault and J.-M. Launay, in *Theory of Chemical Reaction Dynamics* (Kluwer Academic Publishers, Dordrecht, Boston, 2004).

[7] V. Aquilanti and S. Tonzani, J. Chem. Phys. **120**, 4066 (2004).

[8] G. Nyman and H.-G. Yu, Rep. Prog. Phys. **63**, 1001 (2000).

[9] S. Althorpe, in *The Encyclopedia of Computational Chemistry*, edited by P. Schleyer (Wiley, Athens, 2005).

[10] W. Hu and G. C. Schatz, J. Chem. Phys. **125**, 132301 (2006).

[11] B. Lepetit, D. Wang and A. Kuppermann, J. Chem. Phys. **125**, 133505 (2006).

[12] X. Q. Zhang, Q. Cui, J. Z. H. Zhang, and K. L. Han, J. Chem. Phys. **126**, 234304 (2007).

[13] D. De Fazio, V. Aquilanti, S. Cavalli, A. Aguilar, and J. M. Lucas, J. Chem. Phys. **129**, 064303 (2008).

[14] R. N. Porter and L. M. Raff, *Modern Theoretical Chemistry: Dynamics of Molecular Collisions*, edited by W. H. Miller (Plenum Press, New York, 1976), Vol. 2, Part B, p. 1.

[15] D. G. Truhlar and J. T. Muckerman, in *Atom-Molecule Collision Theory: A Guide for the Experimentalist*, edited by R. B. Bernstein (Plenum Press, New York, 1979), p. 505.

[16] T. D. Sewell and D. L. Thompson, Int. J. Mod. Phys. B **11**, 1067 (1997).
[17] M. Karplus, R. N. Porter, and R. D. Sharma, J. Chem. Phys. **40**, 2033 (1964).
[18] N. C. Blais and D. L. Bunker, J. Chem. Phys. **37**, 2713 (1962), and further works by the same authors.
[19] D. Secrest and B. R. Johnson, J. Chem. Phys. **45**, 4556 (1966).
[20] W. H. Miller, J. Chem. Phys. **53**, 1949 (1970).
[21] W. H. Miller, J. Chem. Phys. **53**, 3578 (1970).
[22] W. H. Miller, Chem. Phys. Lett. **7**, 431 (1970).
[23] W. H. Miller, J. Chem. Phys. **54**, 5386 (1971).
[24] C. C. Rankin and W. H. Miller, J. Chem. Phys. **55**, 3150 (1971).
[25] T. F. George and W. H. Miller, J. Chem. Phys. **56**, 5637 (1972).
[26] T. F. George and W. H. Miller, J. Chem. Phys. **56**, 5668 (1972).
[27] T. F. George and W. H. Miller, J. Chem. Phys. **56**, 5722 (1972).
[28] T. F. George and W. H. Miller, J. Chem. Phys. **57**, 2458 (1972).
[29] J. D. Doll and W. H. Miller, J. Chem. Phys. **57**, 5019 (1972).
[30] J. D. Doll, T. F. George, and W. H. Miller, J. Chem. Phys. **58**, 1343 (1973).
[31] W. H. Miller and A. W. Raczkowski, Faraday Discuss. Chem. Soc. **55**, 45 (1973).
[32] W. H. Miller, Adv. Chem. Phys. **25**, 69 (1974).
[33] W. H. Miller, Adv. Chem. Phys. **30**, 77 (1975).
[34] R. A. Marcus, Chem. Phys. Lett. **7**, 525 (1970).
[35] R. A. Marcus, J. Chem. Phys. **54**, 3965 (1971).
[36] J. N. L. Connor and R. A. Marcus, J. Chem. Phys. **55**, 5636 (1971).
[37] W. H. Wong and R. A. Marcus, J. Chem. Phys. **55**, 5663 (1971).
[38] R. A. Marcus, J. Chem. Phys. **56**, 311 (1972).
[39] R. A. Marcus, J. Chem. Phys. **56**, 3548 (1972).
[40] J. R. Stine and R. A. Marcus, Chem. Phys. Lett. **15**, 536 (1972).
[41] R. A. Marcus, Faraday Discuss. Chem. Soc. **55**, 34 (1973).
[42] R. A. Marcus, J. Chem. Phys. **57**, 4903 (1972).
[43] R. A. Marcus, J. Chem. Phys. **59**, 5135 (1973).
[44] J. R. Stine and R. A. Marcus, J. Chem. Phys. **59**, 5145 (1973).
[45] H. Kreek and R. A. Marcus, J. Chem. Phys. **61**, 3308 (1974).
[46] H. Kreek, R. L. Ellis, and R. A. Marcus, J. Chem. Phys. **61**, 4540 (1974).
[47] J. R. Stine and R. A. Marcus, Chem. Phys. Lett. **29**, 575 (1974).
[48] R. Schinke, Theor. Chem. Acc. **103**, 297 (2000).
[49] M. S. Child, *Molecular Collision Theory* (Academic Press, New York, 1974).
[50] M. S. Child, *Semiclassical Mechanics with Molecular Applications* (Oxford University Press, USA, 1991).
[51] J. W. Duff and D. G. Truhlar, Chem. Phys. **4**, 1 (1974).
[52] J. M. Bowman and A. Kuppermann, J. Chem. Phys. **59**, 6524 (1973).
[53] S. C. Cohen and M. H. Alexander, J. Chem. Phys. **61**, 3967 (1974).
[54] M. C. Gutzwiller, *Chaos in Classical and Quantum Mechanics* (Springer-Verlag, New York, 1990).
[55] H.-J. Stöckmann, *Quantum Chaos. An Introduction* (Cambridge University Press, Cambridge, England, 1999).
[56] P. Cvitanović, R. Artuso, R. Mainieri, G. Tanner, G. Vattay, N. Whelan, and A. Wirzba, *Classical and Quantum Chaos*, Chaos Book. org, version 11, 2005, part II.
[57] V. P. Maslov and M. V. Fedoriuk, *Semi-classical Approximations in Quantum Mechanics* (Reidel, Boston, 1981).
[58] R. Blümel and U. Smilansky, Phys. Rev. Lett. **60**, 477 (1988).
[59] G. Campolieti and P. Brumer, J. Chem. Phys. **96**, 5969 (1992).
[60] G. van de Sand and J. M. Rost, J. Phys. B **33**, 1423 (2000).
[61] C. H. Dasso, M. I. Gallardo, and M. Saraceno, Phys. Rev. C **75**, 054611 (2007).
[62] To our knowledge, Marcus was the first to explicitly introduce a phase index in a SCIVR treatment [43] and in CSMT [47]. The index of the SCIVR treatment seems to be justified. However, we have not been able to clearly figure out if this index is equivalent to the Maslov index at constant energy derived later in this work. As far as the CSMT index is concerned [47], we did not find any clear justification of its introduction.
[63] M. C. Gutzwiller, J. Math. Phys. **8**, 1979 (1967).
[64] D. E. Skinner and W. H. Miller, Chem. Phys. Lett. **300**, 20 (1999).
[65] W. H. Miller, J. Phys. Chem. A **105**, 2942 (2001).
[66] M. F. Herman and E. Kluk, Chem. Phys. **91**, 27 (1984).
[67] S. Garashchuk, F. Grossmann, and D. J. Tannor, J. Chem. Soc., Faraday Trans. **93**, 781 (1997).
[68] D. V. Shalashilin and B. Jackson, Chem. Phys. Lett. **291**, 143 (1998).
[69] Y. Elran and K. G. Kay, J. Chem. Phys. **114**, 4362 (2001).
[70] Y. Elran and K. G. Kay, J. Chem. Phys. **116**, 10577 (2002).
[71] L. Bonnet and J.-C. Rayez, Chem. Phys. Lett. **277**, 183 (1997).
[72] L. Bonnet and J.-C. Rayez, Chem. Phys. Lett. **397**, 106 (2004).
[73] L. Bonnet, J. Chem. Phys. **128**, 044109 (2008).
[74] L. Bañares, F. J. Aoiz, P. Honvault, B. Bussery-Honvault, and J.-M. Launay, J. Chem. Phys. **118**, 565 (2003).
[75] T. Xie, J. Bowman, J. W. Duff, M. Braunstein, and B. Ramachandran, J. Chem. Phys. **122**, 014301 (2005).
[76] M. L. González-Martinez, L. Bonnet, P. Larrégaray, and J.-C. Rayez, J. Chem. Phys. **126**, 041102 (2007).
[77] M. L. González-Martínez, W. Arbelo-Gonzalez, J. Rubayo-Soneira, L. Bonnet, and J.-C. Rayez, Chem. Phys. Lett. **463**, 65 (2008).
[78] H. Goldstein, *Classical Mechanics* (Addison-Wesley, Reading, MA, 1950).
[79] S. T. Thornton and J. B. Marion, *Classical Dynamics of Particles and Systems* (Harcourt Brace Jovanovitch, San Diego, 1988).
[80] R. Schinke, *Photodissociation Dynamics* (Cambridge University Press, Cambridge, England, 1995).
[81] P. Pechukas, Phys. Rev. **181**, 166 (1969).
[82] S. Levit and U. Smilansky, Ann. Phys. **103**, 198 (1977).
[83] S. Levit and U. Smilansky, Ann. Phys. **108**, 165 (1977).
[84] S. Levit, K. Möhring, U. Smilansky, and T. Dreyfus, Ann. Phys. **114**, 223 (1978).
[85] G. Campolieti and P. Brumer, Phys. Rev. A **50**, 997 (1994).
[86] G. Campolieti and P. Brumer, Phys. Rev. A **53**, 2958 (1996).
[87] R. G. Littlejohn, J. Stat. Phys. **68**, 7 (1992).
[88] K. Möhring, S. Levit, and U. Smilansky, Ann. Phys. **127**, 198 (1980).

[89] B. Eckhardt and D. Wintgen, J. Phys. A **24**, 4335 (1991).

[90] M. Tabor, *Chaos and Integrability in Non linear Dynamics* (John Wiley and Sons, New York, 1989).

[91] Anyway, CSMT should not be valid when j_{max} is too low, even with g taken into account, for we are in highly quantum conditions.

[92] C. Cohen-Tannoudji, B. Diu, and F. Laloë, *Mécanique Quantique* (Hermann, Paris, 1977), see p. 1462.

[93] H.-D. Meyer, U. Manthe, and L. S. Cederbaum, Chem. Phys. Lett. **165**, 73 (1990).

[94] U. Manthe, H.-D. Meyer, and L. S. Cederbaum, J. Chem. Phys. **97**, 3199 (1992).

[95] M. H. Beck, A. Jäckle, G. A. Worth, and H.-D. Meyer, Phys. Rep. **324**, 1 (2000).

[96] H.-D. Meyer and G. A. Worth, Theor. Chem. Acc. **109**, 251 (2003).

[97] It is a tradition, motivated by historical reasons, to use the expression single particle function, but an alternative terminology might be single degree-of-freedom function.

[98] D. Neuhauser, Chem. Phys. Lett. **200**, 173 (1992).

[99] L. Bonnet, Ann. Phys. **314**, 99 (2004).

[100] V. S. Filinov, Nucl. Phys. B **271**, 717 (1986).

[101] R. D. Coalson, D. L. Freeman, and J. D. Doll, J. Chem. Phys. **85**, 4567 (1986).

[102] N. Makri and W. H. Miller, Chem. Phys. Lett. **139**, 10 (1987).

[103] Available at the following webpage: http://www.pci.uni-heidelberg.de/cms/mctdh.html.